Pertanika Journal of Science & Technology

VOLUME NO. 33
ISSUE NO. 3
SEPT- DEC 2025



ENRICHED PUBLICATIONS PVT. LTD

S-9, IInd FLOOR, MLU POCKET,
MANISH ABHINAV PLAZA-II, ABOVE FEDERAL BANK,
PLOT NO-5, SECTOR-5, DWARKA, NEW DELHI, INDIA-110075,
PHONE: - + (91)-(11)-47026006

Pertanika Journal of Science & Technology

Aim & Scope

AIM

Pertanika Journal of Science & Technology is an official journal of Universiti Putra Malaysia. It is an open-access online scientific journal. It publishes original scientific outputs. It neither accepts nor commissions third party content.

Recognised internationally as the leading peer-reviewed interdisciplinary journal devoted to the publication of original papers, it serves as a forum for practical approaches to improve quality on issues pertaining to science and engineering and its related fields.

Pertanika Journal of Science and Technology is now published in English and it is open for submission by authors from all over the world. It is currently published 6 times a year, in January, March, April, July, August, and October.

Editor-in-Chief

Luqman Chuah Abdullah (Prof. Dr.)

Chemical EngineeringUniversiti Putra Malaysia, Malaysia

Associate Editor

Miss Laiha Mat Kiah

(Prof. Ts. Dr.)Security Services Sn: Digital Forensic, Steganography, Network Security, Information Security, Communication Protocols, Security ProtocolsUniversiti Malaya, Malaysia.

Saidur Rahman

(Prof. Dr.)Renewable Energy, Nanofluids, Energy Efficiency, Heat Transfer, Energy Policy Sunway University, Malaysia.

Chief Executive Editor

To Be Appointed

International Advisory Board

| Hiroshi Uyama (Prof. Dr.) Moha | me |
|--------------------------------|----|

Polymer Chemistry, Organic Compounds, Coating, Chemical Engineering Osaka University, Japan.

Mohamed Pourkashanian (Prof. Dr.)

Mechanical Engineering, Energy, CFD and Combustion Processes Sheffield University, United Kingdom.

Mohini Sain (Prof. Dr.)

Material Science, Biocomposites, Biomaterials University of Toronto, Canada.

Yulong Ding (Prof. Dr.)

Particle Science & Thermal Engineering University of Birmingham, United Kingdom.

Editors

Abdul Latif Ahmad (Prof. Ir. Dr)

Chemical Engineering Universiti Sains Malaysia, Malaysia.

Ahmad Zaharin Aris (Prof. Dr.)

Hydrochemistry, Environmental Chemistry, Environmental Forensics, Heavy Metals Universiti Putra Malaysia, Malaysia.

Azlina Harun@Kamaruddin (Prof. Datin Dr)

Enzyme Technology, Fermentation Technology Universiti Sains Malaysia, Malaysia.

Bassim H. Hameed (Prof. Dr.)

Chemical Engineering: Reaction Engineering, Environmental Catalysis & Adsorption Qatar University, Qatar.

Biswajeet Pradhan (Prof. Dr.)

Digital image processing, Geographical Information System (GIS), Remote Sensing University of Technology Sydney, Australia.

Ho Yuh-Shan (Prof. Dr.)

Water research, Chemical Engineering and Environmental studies Asia University, Taiwan.

| Hsiu-Po Kuo (Prof. Dr.) Chemical Engineering National Taiwan University, Taiwan. | Ivan D. Rukhlenko (Prof. Dr.) Nonliner Optics, Silicon Photonics Plasmonics and Nanotechnology The University of Sydney, Australia. |
|---|---|
| Lee Keat Teong (Prof. Dr.) Energy Environment, Reaction Engineering, Waste Utilization, Renewable Energy Universiti Sains Malaysia, Malaysia. | Mohamed Othman (Prof. Dr.) Communication Technology and Network, Scientific Computing Universiti Putra Malaysia, Malaysia. |
| Mohd Shukry Abdul Majid (Assoc. Prof. Ir. Dr) Polymer Composites, Composite Pipes, Natural Fibre Composites, Biodegradable Composites, Bio-Composites Universiti Malaysia Perlis, Malaysia. | Mohd Zulkifly Abdullah (Prof. Ir. Dr) Fluid Mechanics, Heat Transfer, Computational Fluid Dynamics (CFD) Universiti Sains Malaysia, Malaysia. |
| Mohd. Ali Hassan (Prof. Dr.) Bioprocess Engineering, Environmental Biotehnology Universiti Putra Malaysia, Malaysia | Nor Azah Yusof (Prof. Dr.) Biosensors, Chemical Sensor, Functional Material Universiti Putra Malaysia, Malaysia. |
| Norbahiah Misran (Prof. Dr.) Communication Engineering Universiti Kebangsaan Malaysia, Malaysia. | Roslan Abd-Shukor (Prof. Dato' Dr.) Physics & Materials Physics, Superconducting Materials Universiti Kebangsaan Malaysia, Malaysia. |
| Sodeifian Gholamhossein (Prof. Dr.) Supercritical technology, Optimization, nanoparticles, polymer nanocomposites University of Kasham, Iran | Wing Keong Ng (Prof. Dr.) Aquaculture, Aquatic Animal Nutrition, Aqua Feed Technology Universiti Sains Malaysia, Malaysia. |

Pertanika Journal of Science & Technology

(Volume No. 33, Issue No. 3, Sept- Dec 2025)

Contents

| No. | Articles/Authors Name | Pg. No. |
|-----|---|---------|
| 1 | Dark Fermentative Biohydrogen Production from Palm oil Mill Effluent: | 1 - 15 |
| | Operation Factors and Future Progress of Biohydrogen Energy | |
| | -Fatin Sakinah Rosman1, Mohd Zulkhairi Mohd Yusoff1,2*, Mohd Rafein | |
| | Zakaria1,3, Toshinari Maeda4 and Mohd Ali Hassan1 | |
| 2 | Nutritional Characteristics of Biochar from Pineapple Leaf Residue and | 16 - 27 |
| | Sago Waste | |
| | - Norshidawatie Bohari1,2, Hasmah Mohidin1,2*, Juferi Idris3,4, Yoshito | |
| | Andou5, Sulaiman Man1,2, Hushairy Saidan3 and Suraiya Mahdian1,6 | |
| 3 | Static Mechanical, Thermal Stability, and Interfacial Properties of | 28 - 38 |
| | Superheated Steam Treated Oil Palm Biomass Reinforced Polypropylene | |
| | Biocomposite | |
| | - Muhammad Nazmir Mohd Warid1, Tengku Arisyah Tengku Yasim-Anuar1, | |
| | Hidayah Ariffin1,2*, Mohd Ali Hassan1, Yoshito Andou3 and Yoshihito | |
| | Shirai3 | |
| 4 | Parameters Optimization in Compression Molding of Ultra high Molecular | 39 - 54 |
| | Weight Polyethylene/Cellulose Nanofiber Bio nanocomposites by using | |
| | Response Surface Methodology | |
| | - Nur Sharmila Sharip1, Hidayah Ariffin1,2*, Yoshito Andou3, Ezyana | |
| | Kamal Bahrin2, Mohammad Jawaid4, Paridah Md Tahir5 and Nor Azowa | |
| | Ibrahim6 | |

Dark Fermentative Biohydrogen Production from Palm oil Mill Effluent: Operation Factors and Future Progress of Biohydrogen Energy

Fatin Sakinah Rosman1, Mohd Zulkhairi Mohd Yusoff1,2*, Mohd Rafein Zakaria1,3, Toshinari Maeda4 and Mohd Ali Hassan1

1Department of Bioprocess Technology, Faculty of Biotechnology and Biomolecular Sciences, Universiti Putra Malaysia, 43400 Serdang, Selangor, Malaysia 2Laboratory of Biopolymer and Derivatives, Institute of Tropical Forestry and Forest Products (INTROP), Universiti Putra Malaysia, 43400 UPM Serdang, Selangor, Malaysia

3Laboratory of Processing and Product Development, Institute of Plantation Studies, Universiti Putra Malaysia, 43400, UPM Serdang, Selangor, Malaysia 4Department of Biological Functions and Engineering, Graduate School of Life Science and Systems

Engineering, Kyushu Institute of Technology, 2-4 Hibikino, Wakamatsu-ku, Kitakyushu, Fukuoka 808-0196, Japan

ABSTRACT

Malaysia is one of the largest producers and exporters of palm oil, thus, a large amount of palm oil mill effluent (POME) is generated through this process. POME contributes to environmental pollution if it is not properly treated. This complex effluent consists of colloidal matters and mainly organic components with more than 90% water. Thus, it is useful to be used as a substrate for fermentative processes, including biohydrogen production. Biohydrogen from POME is a renewable source that can potentially serve as an alternative to substitute fossil fuels. The abundance of POME and the rising price of fossil fuels in the global market create a demand for this source of energy. However, the complexity of the substituents in POME makes the optimisation of this effluent as a substrate in dark fermentation a challenge. This review article explores the important parameters that need to be considered for optimal biohydrogen production, such as the bioreactor operational parameters and the microbial consortium. Besides, the potential of metabolic engineering as a tool to overcome the limitations of the microbial strains to metabolise POME for increased biohydrogen production was also reviewed. However, further research and development are needed to increase the biohydrogen yield on par with commercial demand.

Keywords: Biohydrogen, dark fermentation, hydrogen-producing microorganisms, palm oil mill effluent

INTRODUCTION

As the availability of fossil fuels is steadily decreasing over the years, a renewable alternative source of energy needs to be considered. Biohydrogen is one of the potential replacements of fossil fuels. Biohydrogen refers to hydrogen that has been generated through biological processes (Kapdan & Kargi, 2006). Biohydrogen is a clean energy source and considered renewable since it can be produced

continuously from various renewable sources such as oil palm biomass and food waste (Mohd Yasin et al., 2013). This gas is odourless, colourless, combustible, and nontoxic. Unlike hydrocarbon fuels, hydrogen gas burns cleanly without emitting any environmental pollutants. This is because hydrogen combustion only produces water vapour (H2 O) (Mokhtar et al., 2019).

Table 1 shows the comparison between gasoline, ethanol, methane, and hydrogen, respectively as energy carriers. Biohydrogen is also an interesting biofuel since it is scaleindependent and has a high conversion rate to electricity via fuel cells compared to other gaseous fuels (Groot, 2003). According to the International Energy Agency (IEA), in 2018, the cost of hydrogen gas production from renewable sources is approximately USD 3.07.5/kg, while the cost of using coal as a feedstock is about USD 1.2-2.2/kg of hydrogen (IEA, 2020). In 2020, it can be seen that the prices of alternative fuels (biodiesel B20 USD 2.36/gallon, biodiesel B99-B100 USD 3.51/gallon) are comparative to hydrocarbon fuels (diesel USD 2.61/gallon and gasoline USD 1.91/gallon) (Energy, 2020).

In order to make the production of biohydrogen more sustainable and cost-effective, the use of renewable resources as the feedstock is more ideal compared to the conventional simple sugars. Thus, in conjunction with a sustainable and environmentally friendly strategy, many researchers have preferred to utilise organic biomass as alternative substrates for biohydrogen production.

The POME generated will be utilised by anaerobic microorganisms in a bioreactor as a substrate to generate biohydrogen through a process called dark fermentation. Thus, to take full advantage of this inexhaustible resource, the efficiency of the dark fermentation process by the microbes needs to be optimised. Therefore, this review also covers the crucial factors that may contribute to the efficiency of biohydrogen production through dark fermentation. This includes microbial limitation, environmental limitation, operational condition, and the application of metabolic engineered microorganisms. The current development and future projection of biohydrogen production from the renewable substrate were discussed thoroughly.

Table 1 Properties of energy carriers; H₂, CH₄, ethanol, and gasoline

| Energy Carrier Properties | Hydrogen | Methane | Ethanol | Gasoline |
|--|----------|----------|---------|-----------|
| Density, gas (NTP) (kg m ³⁻¹) | 0.0899 | 0.651 | N.A. | N.A. |
| Density, liquid (kg m3-1) | 70.8 | 422.6 | 789.3 | 720 - 780 |
| Melting point (°C) | -259.1 | -182.3 | -114.15 | -40 |
| Boiling point (°C) | -252.76 | -161.15 | 78.29 | N.A. |
| Lower heating value (MJ kg ⁻¹) | 119.9 | 50.0 | N.A. | 44.6 |
| Energy per unit mass (MJ kg-1)* | 141.9 | 55.5 | 29.9 | 47.4 |
| Energy per unit volume (GJ m3-1) | 0.013 | 0.651 | 23.6 | 34.85 |
| Flame temperature (°C) | 2045 | 1875 | N.A. | 2200 |
| Self-ignition temperature (°C) | 585 | 540 | 423 | 228-501 |
| Minimal ignition energy (mJ) | 0.2 | 0.29 | N.A. | 0.24 |
| Ignition limits in air (vol %) | 4 - 75 | 5.3 - 15 | 4.3 -19 | 1.0 - 7.6 |
| Flame propagation in air (m s-1) | 2.65 | 0.4 | N.A. | 0.4 |
| Diffusion coefficient in air (cm2 s-1) | 0.61 | 0.16 | N.A. | 0.05 |
| Toxicity | No | No | No | Yes |
| N.A. = not available | | | | |

Sources: (Najafpour et al., 2015: Xu et al., 2009)

Substrate for Biohydrogen Production via Dark Fermentation

The increasing trend in palm oil production gains the concern of environmental activist groups. This is because palm oil plantation expansion leads to deforestation, causing loss of biodiversity. An increase in palm oil production also reflected the increase in crude palm oil (CPO) production. CPO production becomes an environmental issue due to the massive generation of POME from the process of CPO extraction where a tonne of CPO produces approximately 3.05 tonnes of POME (Singh et al., 2010). POME is the largest wastewater produced and the most problematic environmental pollutant in the palm oil industry (Singh et al., 2010). This complex effluent is viscous, brownish in colour, and consists of colloidal matters, with more than 90% of water. The solids content of POME comprises more than 5% total solids and around 4% suspended solids (Taifor et al., 2017). The POME also has a discharge temperature of 80–90°C.

The pre-treatment of POME is vital before its utilisation, not only as a substrate for biohydrogen production through microbial fermentation but also for the production of various products such as biosolvents (Hipolito et al., 2008), bioacids (Mumtaz et al., 2008) and polyhydroxyalkanoates (PHA) (Hassan et al., 1997). The alkaline-heat supernatant pretreatment was shown to produce the highest biohydrogen production (2.18 mol H2 /mol total carbohydrate) by POME compared to other pretreatment like acid (Kamal et al., 2012).

MATERIALS AND METHODS

General Factors that Influence Biohydrogen Productivity: Nutrients Macronutrients and micronutrients are essential in dark fermentation which includes: carbon and nitrogen sources (Lin & Lay, 2004a), ammonium, phosphate (Lin & Lay, 2004b), sulphur, sulphate (Cheng et al., 2011), iron (Yang & Shen, 2006), and elemental traces (Lin & Lay, 2005). The concentration of these nutrients also influences the growth of microbes and hydrogen production. The ranges of nitrogen concentration around 0.1-2.0 g N/L with a C/N ratio of 3.3 to 130 were found to result in optimal growth.

Besides microbial growth, the efficiency of biohydrogen production also relies on the microbial hydrogenases that are involved in hydrogen metabolism. The most important element that influences the action of hydrogenases is ferredoxin (Chou et al., 2007). This is because iron is important for hydrogenase activity and may deviate the fermentation pathways away from biohydrogen production (Yang & Shen, 2006). Reported that magnesium, sodium, and zinc were reported as the most significant elements for biohydrogen production. The optimum concentrations of elements were (mg/L) 0.25 Zn2+, 4.8 Mg2+, 1 Fe2+ and 393 Na+. The maximum biohydrogen yield was 233 mL H2 /g/hexose from sucrose-containing wastewater (Lin & Lay, 2005).

Buffer. Organic acids are by-products produced from the dark fermentation of biohydrogen production. The accumulation of these acids will reduce the pH of the growth medium of the microbes, resulting in a

decrease in biohydrogen production or stunting the microbial growth. Therefore, a strong buffer in the medium is required to oppose the pH change caused by organic acids produced. Carbonate buffers (NaHCO3 and Nh4 Co3) are widely used in biohydrogen dark fermentation studies. However, the use of these buffers may result in the formation of additional Co2 due to the interaction of HCO3 with acidic metabolites (Lin & Lay, 2005). This situation should be avoided as the gas build-up will induce toxicity of the microbial environment. Hence, the use of phosphate buffer is preferable to alleviate this concern. This is because some studies have found that the use of phosphate buffers like K2 HPO4 and Na2 HPO4 could maintain the pH values of the medium and promote hydrogen production (Lin et al., 2011).

Hydrogen Partial Pressure. The theory predicts that by reducing the partial pressure of hydrogen may increase the biohydrogen yields from glycerol. High dissolved H2 concentration in the culture medium inhibits H2 production and favour the hydrogen consumption pathway instead (Mandal et al., 2006). Immediate removal of H2 from the culture medium is recommended to facilitate maximum H2 yields that showed hydrogen yield was doubled to 3.9 mol H2 /mol glucose (Chong et al., 2009). Another method that can be employed is by adding chemicals like KOH and NaOH, to absorb carbon dioxide from the headspace and by removing the dissolved gases (Saady, 2013). The addition of the chemicals will create a vacuum environment. However, the addition of the chemicals will increase the pH of the medium, thus, affecting the optimal pH needed to maintain bacterial growth. Agitation served to remove dissolved gases such as Co2 and H2 from the fermentation medium. Ferchichi et al. (2005) revealed the agitation up to 100 rev/min yielded 1.66 mol-H2/mol.

Limitation of Dark Fermentation for Biohydrogen Production

Physicochemical Conditions. Table 2 depicts the advantages, disadvantages, mechanisms of biohydrogen production through dark fermentation. The metabolism of bacteria for biohydrogen production through dark fermentation is highly dependent on the physicochemical factors. Among the crucial factors are the pH, hydraulic retention time, partial pressure of hydrogen, temperature, fermentation products, by-products inhabitation and growth media.

Table 2
Microbial biohydrogen production mechanisms by dark fermentation: advantages and disadvantages

| Mechanism | $C_6H_{12}O_6 + 2H_2O \rightarrow 2CH_3COOH + 4H_2 + 2CO_2$ |
|---------------|--|
| Advantages | H₂ production from various carbohydrates and organic wastes High H₂ production rates No light required Simpler process for engineering than the others H₂ can be produced along with the high-value compounds (e.g.: glucogenic acid and 1,3-propanediol) |
| Disadvantages | CO₂ present in the product gas Incomplete oxidisation of organic materials to H₂, low H₂ yields Effluent treatment required Impurity of product gas, traces of H₂S, methane and carbon dioxide. |

Substrate Inhibition. The mechanisms of biohydrogen production involving microbes are catalysed by mainly hydrogenase and nitrogenase enzymes (Vignais et al., 2006). Both mechanisms utilise the presence of protons as the electron sink during the metabolism of organic substrates that act as electron donors. The nitrogenase enzyme catalyses the reduction of nitrogen gas to ammonia (Tamagnini et al., 2002). The absence of N2 will, therefore, shift the total electron flux to biohydrogen production instead. This reaction is irreversible and can produce biohydrogen even at saturated biohydrogen concentration in the medium and this reaction is energy-intensive (Vignais et al., 2006).

The hydrogenases can be distinguished based on the types of electron donors and acceptors used in hydrogen metabolisms such as NAD, cytochrome, coenzyme, and ferredoxins. The enzymes can also be classed based on the metallic cofactors and sequence similarity of the hydrogenases. There are currently three known classes: [NiFe]hydrogenases (Forzi & Sawers, 2007), [FeFe]-hydrogenases and [Fe]-hydrogenases (Fang et al., 2017). Interestingly, it was found that the functionality of the different Hyd enzymes largely depending on the pH (Sanchez-Torres et al., 2013). The majority of studies on biohydrogen production involves the metabolism of simple sugars. POME is a complex substance which could not be readily available for microbes to metabolise. It leads to long adaptive phases and low conversion rates into the product. However, the components of the complex substrates will be transformed into simple compounds through the degradation process. The stoichiometric reactions involved in the dark fermentation were explicated in Table 3.

1able 3
Stoichiometries reaction of dark fermentation of glucose for biohydrogen production

| Reaction | Stoichiometry | ΔG0' (kJ reaction) | Reference | |
|-----------------------------------|---|--------------------|-------------------------|--|
| Oxidation of glucose | $C_6H_{12}O_6 + 12H_2O \rightarrow 12H_2 + 6HCO_3 + 6H^+$ | + 3.2 | | |
| Acetate production | $\begin{array}{l} C_6H_{12}O_6+4H_2O \rightarrow 2CH_3COO^{\cdot}+4H_2+2HCO_3^{\cdot} \\ +4H^{+} \end{array}$ | - 206.3 | (0) | |
| Butyrate production | $ \begin{array}{l} C_6H_{12}O_6+2H_2O \rightarrow CH_3CH_2CH_2COO^-+2H_2+ \\ 2HCO_3^-+3H^+ \end{array} $ | - 254.8 | (Chou et al., 2008) | |
| Ethanol production | $C_6H_{12}O_6 + 2H_2O \rightarrow 2CH_3CH_2OH + 2HCO_3^- + 2H^+$ | - 235.0 | | |
| Acetate and ethanol Production | $C_6H_{12}O_6 + 3H_2O \rightarrow CH_3CH_2OH + CH_3COO^- + 2H_2 + 2HCO_3^- + 3H^+$ | - 215.716 | (Hwang et al., 2004) | |
| Lactate production | $C_6H_{12}O_6 \rightarrow 2CH_3CHOHCOO^{\cdot} + 2H^{\scriptscriptstyle +}$ | - 198.1 | (Kim et al., 2009) | |
| Butanol production | $C_6H_{12}O_6 + H_2O \rightarrow CH_3CH_2CH_2OH + 2HCO_3^- + 2H^+$ | - 280.5 | (Chin et al., 2003) | |
| Propionate production | $C_6H_{12}O_6 + 2H_2 \longrightarrow 2CH_3CH_2COO^{\scriptscriptstyle \circ} + 2H_2O + 2H^{\scriptscriptstyle +}$ | - 359.0 | (Morimoto et al., 2005) | |
| Valerate production | $C_6H_{12}O_6 + H_2 \rightarrow CH_3CH_2CH_2CH_2COO^{-} + HCO_3^{-} + H_5O + 2H^{+}$ | | (Chou et al., | |
| Acetogenesis | $4H_2 + 2HCO_3^- + H^+ \rightarrow CH_3COO^- + 4H_2O$ | - 104.6 | 2008) | |
| Acidogenesis | $C_6H_{12}O_6 \rightarrow 3CH_3COO^{\scriptscriptstyle \circ} + 3H^{\scriptscriptstyle +}$ | - 310.6 | (Kim et al., 2009) | |

Temperature. The temperature influences the microbial growth and consequently increases enzymatic reactions and the rate of chemical synthesis (Dasgupta et al., 2010). Dark fermentation metabolism can occur within a wide range of temperatures 15-45°C (mesophilic), hyper-thermophilic (more than 80°C). Previous studies on the production of biohydrogen under thermophilic conditions were compared in Table 4.

The effects of temperature from mesophilic to thermophilic (25 - 55°C) during the fermentation were investigated by Yossan et al. (2012) and the results showed that the

Table 4

Advantages and disadvantages of biohydrogen dark fermentation in thermophilic condition

Advantages Increase in the rates of chemical and enzymatic reactions Increase in thermodynamic favourability of H₂-production. H₂ production becomes less affected by the partial pressure of H₂. The solubility of H₂ and CO₂ to water decreases Reactors are less prone to contamination by H₂-consuming organisms Decreased diversity of side products Some thermophiles excrete exoenzymes, which can hydrolyze biopolymers Suitable for direct processing high-temperature wastewaters Destruction of pathogens in the reactor effluent

Source: (Hallenbeck, 2005; Hawkes et al., 2002)

biohydrogen yield was optimum at 37°C. The highest yield of biohydrogen was obtained using 55°C reactor temperature with 985.3 mL/L POME. O-thong et al. (2011) optimised three different temperatures between 35-75°C, which produced the biohydrogen production at 1104 mL H2 /L POME (35°C), and maximum at 4750 mL H2 /L POME (55°C), respectively. Based on the statistical analysis, the optimal condition for biohydrogen production was at 60°C, with a maximum production of biohydrogen at 4820 mL H2 /L POME. These studies have clearly shown that high temperature is the most ideal fermentation temperature to achieve the highest biohydrogen yield using POME.

pH. The optimal growth pH is microbial dependent and an important factor in suppressing the behaviour of the hydrogen-consuming methanogens. Studies showed different initial pH yielded different biohydrogen value, 2584 mL H2/L POME (pH 4.5), 4750 mL H2/L POME (pH 5.5) and 4300 mL H2/L POME (pH 6.5), respectively (O-thong et al., 2011). The optimal initial pH for biohydrogen production was found at 5.5, where the reaction achieved the maximum production of biohydrogen at 4820 mL H2 L/POME. RSM analyses from different studies showed the optimum production of biohydrogen was found at 272 mL H2/g substrate with an initial pH around 5.70. Another experiment using microflora in POME sludge also showed that the maximum biohydrogen production rate was 98 mL H2/h with initial pH at 5.98 (Rasdi et al., 2009).

Under slightly acidic conditions, the bacteria growth of methanogens will be suppressed. The ability of biohydrogen-producing bacteria to develop will be increased. Moreover, controlling the pH in dark fermentation is important because organic acids generated as by-products tend to reduce the pH of the culture medium (Li & Chen, 2007).

Products Inhibition. Biohydrogen is typically produced from the metabolism of glucose or sucrose that also produces secondary products such as acetate and butyrate. The organic acids can reduce the rate of cell growth at lower concentrations and cause changes in cell metabolic process (Kyazze et al., 2006). The organic acids (undissociated) may pass through the cell membrane and dissociate within the cell of

bacteria. This occurs when the pH inside the cell is higher than its surroundings. Therefore, high organic acid concentrations can disrupt the proton motive force (pH gradient) across the cell membrane, resulting in metabolic inhibition (Van Ginkel & Logan, 2005). Thus, biohydrogen production is typically more influenced by the disassociated butyric acid than by acetic acid, due to butyric acid having lower pKa value than acetic acid at 4.7 (Hawkes et al., 2007).

Another end-product which could suppress the biohydrogen production is ethanol. Lack of bacteria tolerance against ethanol. Thermophilic bacteria are less ethanol-tolerant than mesophilic bacteria (Burdette et al., 2002). The most ethanol-tolerant strains are the Thermoanaerobacter sp. strain A10 (Georgieva et al., 2007) and Clostridium sp. strain SS22 (5% (v/v) (Rani & Seenayya, 1999).

Inoculum. Most of the microbes that are studied for biohydrogen production are obligate anaerobes (i.e. Clostridia). However, the combination of facultative anaerobes with obligate anaerobes in the biohydrogen production may create more advantageous (Chong et al., 2009). Several bacteria can metabolise the complex material such as POME into simple sugars or organic acids, while others utilise these intermediate products to produce biohydrogen. The highest yield of biohydrogen was reported to be at 2.15 mol H2/molhexose from 3.2 L anaerobic batch sequencing reactor (ASBR) (O-Thong et al., 2007). In another study, the highest biohydrogen yield was 1773 N mL H2 /L POME using continuous batch. The studies evidenced that mixed cultures are more advantageous compared to pure cultures. Single culture also plays a significant role particularly its metabolism and the optimal growth conditions during biohydrogen production. O-Thong et al. (2009) showed that the Thermoanaerobacterium had produced 25.9 mmol H2 /d from POME. Chong and colleagues found that the Clostridium butyricum EB6 generated 948 mL H2/mL glucose from POME (Chong et al., 2009). Besides, it is also important to reduce the presence of bacteria that may inhibit the production of biohydrogen like methanogens and sulphate reducers. Methanogens may be depleted using shorter hydraulic retention time (HRT), provided that the HRT is not exceeding the crucial value where biohydrogen producing bacteria may be washed out (Ismail et al., 2010).

Metabolic Engineering Approaches

Metabolic engineering is one of the available strategies to address the limitations presented by dark fermentation in the production of biohydrogen. The theoretical biohydrogen yield from dark fermentation using glucose as a carbon source is 12 mol H2 and 6 mol Co2 per mole glucose, but there are no reported natural bacteria that possess the metabolism that is capable to generate this value (Chaudhary et al., 2012). However, based on several known fermentation reactions, the theoretical maximum H2 yield is only 4 mol H2 / mol glucose produced by strictly anaerobic bacteria. Meanwhile, facultative bacteria can only produce biohydrogen yield of 2 mol H2 /mol glucose (Mohd Yasin et al., 2013). Therefore, the theoretical maximum yield represents only 25% of substrate conversion into

biohydrogen, signalling the inefficiency of the system. This is because other metabolic by-products of dark fermentation like butyrate, propionate, ethanol, lactate, including biomass, are also generated in significant amounts (Table 3).

E.coli has been employed as a robust model strain for metabolic engineering and protein engineering to improve the productivity of hydrogen-producing bacteria (Sanchez-Torres et al., 2013). Even though obligate anaerobes like Clostridia spp. showed higher hydrogen production compared to E. coli (Table 5), they require more sophisticated cultivation set-up because they are obligate anaerobes.

Table 5
Types of microorganism, bioreactor types and scales and biohydrogen production from POME through the dark fermentation process

| Microorganism | Hydrogen Yield | Hydrogen Production Rate | Reactor Type | References |
|-------------------------|---|---|---------------|---|
| C. butyricum EB6 | 298 mL H ₂ /g carbohydrate | 849.5 mL H ₂ /h | 3L Reactor | (Chong, Sabaratnam, et al., 2009) |
| Thermoanaerobacterium- | 6.5 L H ₂ /L-POME | 25.9 mmol H ₂ /L/d | 150 mL bottle | (O-Thong et al., 2007) |
| Thermosaccharolyticum | $4.6 L H_2/L$ -POME | - | 1L ASBR | |
| Mixed culture | 199 mmol H ₂ /L- POME | - | 1L Reactor | (O-Thong et al., 2007) |
| Mixed culture | $0.27~L~H_2/g\text{-COD}$ | $9.1 L H_2/L/$ POME/d | 3.2L ASBR | (Prasertsan et al., 2009) |
| Mixed culture | 840 NmL H ₂ /L- POME | 35 N mL/H ₂ /L/ POME/h | 50L CSTR | (Yusoff et al., 2009) |
| Suspended Mixed culture | $145.9 \text{cm}^3 \text{H}_2/\text{g}$ - COD | 240.5 cm ³ H ₂ /g- VSS/d | 122 cm³ vials | (Ismail et al., 2010) |
| Mixed culture | 1054 NmL H ₂ /L- POME | 44 N mL H ₂ /L/ POME/h | 50L CSTR | (Yusoff et al., 2009) |

Maeda and his colleagues designed the robust engineered E. coli strains for enhanced biohydrogen production (Maeda et al., 2008). To date, the framework for metabolic engineering is restricted to the well-described microorganism, limiting the window of opportunity to discover novel genes that may increase the production of biohydrogen.

Future Progress of Dark Fermentation for Biohydrogen Production

The largest obstacle to biohydrogen production using POME was low biohydrogen molar yield, which only reached 10-20% of the total energy the substrate can provide (Angenent et al., 2004). In addition, estimation of the use of POME to produce biohydrogen is determined using simple sugars such as glucose, since it is impossible to measure the moles of complex substrates like POME. Many studies have shown that the lower yield of biohydrogen production through dark fermentation is due to the bioconversion of POME into multiple by-products (Hipolito et al., 2008). The presence of multiple by-products will not only increase the pH of the culture medium but also cause the purification of products more difficult.

Technologies and systems for biohydrogen production are well known, but currently imperfect for

complex substrates. Most of the technical issues are related to the use of stand-alone technology, such as exclusive use of dark fermentation (Levin, 2004). The integrated biohydrogen and methane production system is currently the best solution to these issues. The advantages of the two-stage system include the efficiency of the process, higher yield of biogas and high total energy recovery (Hawkes et al., 2002). Figure 1 shows the emerging POME biohydrogen manufacturing approach using hybrid systems. In the f irst stage, POME will be transformed into organic acids and biohydrogen using dark fermentation, followed by the conversion of the organic acids into biohydrogen via photo fermentation. By implementing this hybrid system, biohydrogen production efficiency increased from the first stage at 50% to 70% in the second stage (Cheng et al., 2011). However, the main problem in the hybrid system is the implementation of the second stage

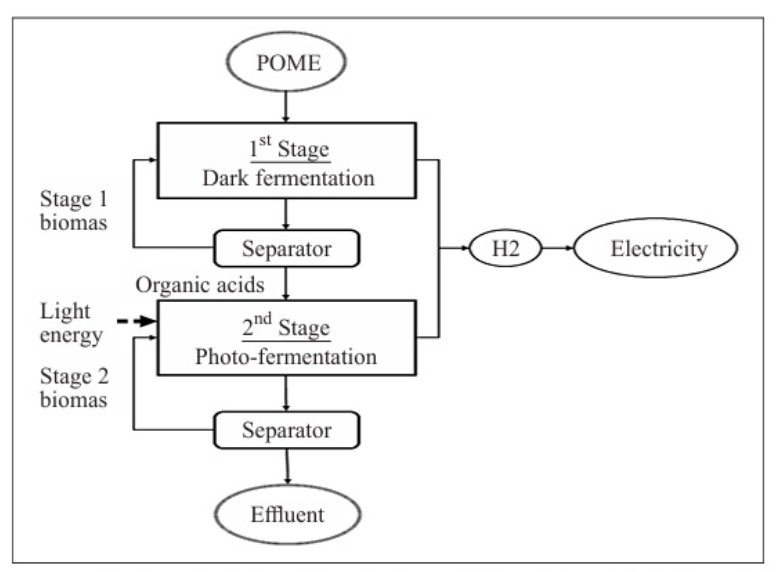


Figure 1. The proposed strategy of an integrated system by combining dark and photo fermentation to produce biohydrogen from POME as a carbon source

(photo fermentation), where it requires high cost and complex infrastructure to set up the photobioreactor (Cheng et al., 2011).

Another method to improve the fermentation flux is through the integration of metabolic engineering of the microbial strains with optimal fermentation parameters. For example, integrating the metabolic engineering and low partial pressure during fermentation process was found to significantly enhance the hydrogen production (Mandal et al., 2006).

However, not many kinds of research have been conducted in pairing metabolic engineering and bioprocessing technology. Most efforts in influencing the metabolic pathway of POME fermentation for biohydrogen production are centred on editing the Fe and Ni hydrogenases pathways as mentioned in another section.

The modification of existing pathways using metabolic engineering approaches will also lead to the creation of a new robust strain with higher hydrogen yield and better productivity. In addition, through metabolic engineering, genetic modification can be made to fully exploit the abundant substrate

availability of POME and its derivatives (Taifor et al., 2017). These strategies can also be applied for other applications to construct recombinant strains to produce a wide range of chemicals and bioproducts. Therefore, the application of the metabolic engineering methods in industrial-scale bioprocessing is a promising study to improve the production of biohydrogen.

CONCLUSION

Dark fermentation is one of the anaerobic fermentation processes applied for biohydrogen production. The performance can be recovered by manipulating the factors that have tremendous influences on biohydrogen production, including pH, temperature, medium formulation, and the application of genetic engineering. Bench studies provide basic essential information to know and understand the microbial limitation, environmental limitation, and operational condition for biohydrogen production. The production strains can be manipulated by genetic engineering to obtain the strains that can utilise POME for biohydrogen production with minimal intermediate products, such as organic acids, solvents, or amino acids. Another important step is to shift the biohydrogen production from bench to pilot scalemostly operated by continuous systems, without compromising the ability of microorganisms to convert complex substrate into biohydrogen. Nevertheless, further investigation from the bench studies and the industry are needed to enhance the efficient utilisation of wastewater, like POME, towards maximal biohydrogen production through dark fermentation.

ACKNOWLEDGEMENTS

The authors would like to acknowledge and thank Universiti Putra Malaysia for the Grant Putra (UPM/700-2/1/GP-IPM/2017/9559800) and the provision of Graduate Research Fund to the first author, Fatin Sakinah Rosman.

REFERENCES

Angenent, L. T., Karim, K., Al-Dahhan, M. H., Wrenn, B. A., & Domiguez-Espinosa, R. (2004). Production of bioenergy and biochemicals from industrial and agricultural wastewater. Trends in Biotechnology, 22(9), 477-485. doi:10.1016/j.tibtech.2004.07.001

Burdette, D. S., Jung, S. H., Shen, G. J., Hollingsworth, R. I., & Zeikus, J. G. (2002). Physiological function of alcohol dehydrogenases and long-chain (C30) fatty acids in alcohol tolerance of Thermoanaerobacter ethanolicus. Applied and Environmental Microbiology, 68(4), 1914-1918. doi:10.1128/aem.68.4.19141918.2002

Chaudhary, N., Ngadi, M. O., & Simpson, B. (2012). Comparison of glucose, glycerol and crude glycerol fermentation by Escherichia Coli K12. Journal of Bioprocessing & Biotechniques, S(01), 1-5.

doi:10.4172/2155-9821.s1-001

Cheng, C. L., Lo, Y. C., Lee, K. S., Lee, D. J., Lin, C. Y., & Chang, J. S. (2011). Biohydrogen production from lignocellulosic feedstock. Bioresource Technology, 102(18), 8514-8523. doi:10.1016/j. biortech.2011.04.059

Cheng, J., Su, H., Zhou, J., Song, W., & Cen, K. (2011). Hydrogen production by mixed bacteria through dark and photo fermentation. International Journal of Hydrogen Energy, 36(1), 450-457. doi:10.1016/j. ijhydene.2010.10.007

Chin, H. L., Chen, Z. S., & Chou, C. P. (2003). Fedbatch operation using Clostridium acetobutylicum suspension culture as biocatalyst for enhancing hydrogen production. Biotechnology Progress, 19(2), 383-388. doi:10.1021/bp0200604

Chong, M. L., Rahim, R. A., Shirai, Y., & Hassan, M. A. (2009). Biohydrogen production by Clostridium butyricum EB6 from palm oil mill effluent. International Journal of Hydrogen Energy, 34(2), 764-771. doi:10.1016/j.ijhydene.2008.10.095

Chong, M. L., Sabaratnam, V., Shirai, Y., & Hassan, M. A. (2009). Biohydrogen production from biomass and industrial wastes by dark fermentation. International Journal of Hydrogen Energy, 34(8), 3277-3287. doi:10.1016/j.ijhydene.2009.02.010

Chou, C. J., Jenney, F. E., Jr., Adams, M. W., & Kelly, R. M. (2008). Hydrogenesis in hyperthermophilic microorganisms: Implications for biofuels. Metabolic Engineering, 10(6), 394-404. doi:10.1016/j. ymben.2008.06.007

Chou, C. J., Shockley, K. R., Conners, S. B., Lewis, D. L., Comfort, D. A., Adams, M. W., & Kelly, R. M. (2007). Impact of substrate glycoside linkage and elemental sulfur on bioenergetics of and hydrogen production by the hyperthermophilic archaeon Pyrococcus furiosus. Applied and Environmental Microbiology, 73(21), 6842-6853. doi:10.1128/aem.00597-07

Fang, X., Sastry, A., Mih, N., Kim, D., Tan, J., Yurkovich, J. T., . . . Palsson, B. O. (2017). Global transcriptional regulatory network for Escherichia coli robustly connects gene expression to transcription factor activities. Proceedings of the National Academy of Sciences, 114(38), 10286-10291. doi:10.1073/pnas.1702581114

Ferchichi, M., Crabbe, E., Hintz, W., Gil, G. H., & Almadidy, A. (2005). Influence of culture parameters on biological hydrogen production by Clostridium saccharoperbutylacetonicum ATCC 27021. World Journal of Microbiology and Biotechnology, 21(6-7), 855-862. doi:10.1007/s11274-004-5972-0

Forzi, L., & Sawers, R. G. (2007). Maturation of [NiFe]-hydrogenases in Escherichia coli. BioMetals, 20(3-4), 565-578. doi:10.1007/s10534-006-9048-5

Georgieva, T. I., Skiadas, I. V., & Ahring, B. K. (2007). Effect of temperature on ethanol tolerance of a thermophilic anaerobic ethanol producer Thermoanaerobacter A10: Modeling and simulation. Biotechnology and Bioengineering, 98(6), 1161-1170. doi:10.1002/bit.21536

Hallenbeck, P. C. (2005). Fundamentals of the fermentative production of hydrogen. Water Science Technology, 52(1-2), 21-29. doi:10.2166/wst.2005.0494

Hassan, M. A., Shirai, Y., Kusubayashi, N., Karim, M. I. A., Nakanishi, K., & Hasimoto, K. (1997). The production of polyhydroxyalkanoate from anaerobically treated palm oil mill effluent by Rhodobacter sphaeroides. Journal of Fermentation and Bioengineering, 83(5), 485-488. doi:10.1016/s0922338x(97)83007-3

Hawkes, F., Hussy, I., Kyazze, G., Dinsdale, R., & Hawkes, D. (2007). Continuous dark fermentative hydrogen production by mesophilic microflora: Principles and progress. International Journal of Hydrogen Energy, 32(2), 172-184. doi:10.1016/j.ijhydene.2006.08.014

Hawkes, F. R., Dinsdale, R., Hawkes, D. L., & Hussy, I. (2002). Sustainable fermentative hydrogen production: Challenges for process optimisation. International Journal of Hydrogen Energy, 27(11-12), 1339-1347. doi:10.1016/s0360-3199(02)00090-3

Hipolito, C. N., Crabbe, E., Badillo, C. M., Zarrabal, O. C., Morales Mora, M. A., Flores, G. P., ... & Ishizaki, A. (2008). Bioconversion of industrial wastewater from palm oil processing to butanol by Clostridium saccharoperbutylacetonicum N1-4 (ATCC 13564). Journal of Cleaner Production, 16(5), 632-638. doi:10.1016/j.jclepro.2007.02.005

Hwang, M. H., Jang, N. J., Hyun, S. H., & Kim, I. S. (2004). Anaerobic bio-hydrogen production from ethanol fermentation: the role of pH. Journal of Biotechnology, 111(3), 297-309. doi:10.1016/j.jbiotec.2004.04.024

IEA. (2020). World energy prices 2020. International Energy Agency. Retrieved October 5, 2020, from https://www.iea.org/reports/energy-prices-2020

Ismail, I., Hassan, M. A., Abdul Rahman, N. A., & Soon, C. S. (2010). Thermophilic biohydrogen production from palm oil mill effluent (POME) using suspended mixed culture. Biomass and Bioenergy, 34(1), 4247. doi:10.1016/j.biombioe.2009.09.009

Kamal, S. A., Jahim, J. M., Anuar, N., Hassan, O., Daud, W. R. W., Mansor, M. F., & Rashid, S. S. (2012). Pre-treatment effect of Palm Oil Mill Effluent (POME) during hydrogen production by a local isolate Clostridium butyricum. International Journal on Advanced Science, Engineering and Information Technology, 2(4), 325-331. doi:10.18517/ijaseit.2.4.214

Kapdan, I. K., & Kargi, F. (2006). Bio-hydrogen production from waste materials. Enzyme and Microbial Technology, 38(5), 569-582. doi:10.1016/j.enzmictec.2005.09.015

Kim, S., Seol, E., Oh, Y. K., Wang, G. Y., & Park, S. (2009). Hydrogen production and metabolic flux analysis of metabolically engineered Escherichia coli strains. International Journal of Hydrogen Energy, 34(17), 7417-7427. doi:10.1016/j.ijhydene.2009.05.053

Kyazze, G., Martinez-Perez, N., Dinsdale, R., Premier, G. C., Hawkes, F. R., Guwy, A. J., & Hawkes, D. L. (2006). Influence of substrate concentration on the stability and yield of continuous biohydrogen

production. Biotechnology Bioengineering, 93(5), 971-979. doi:10.1002/bit.20802

Lee, D. H., Lee, D. J., & Chiu, L. H. (2011). Biohydrogen development in United States and in China: An input—output model study. International Journal of Hydrogen Energy, 36(21), 14238-14244. doi:10.1016/j.ijhydene.2011.05.084

Levin, D. (2004). Biohydrogen production: Prospects and limitations to practical application. International Journal of Hydrogen Energy, 29(2), 173-185. doi:10.1016/s0360-3199(03)00094-6

Li, D., & Chen, H. (2007). Biological hydrogen production from steam-exploded straw by simultaneous saccharification and fermentation. International Journal of Hydrogen Energy, 32(12), 1742-1748. doi:10.1016/j.ijhydene.2006.12.011

Lin, C. Y., & Lay, C. H. (2004a). Carbon/nitrogen-ratio effect on fermentative hydrogen production by mixed microflora. International Journal of Hydrogen Energy, 29(1), 41-45. doi:10.1016/s0360-3199(03)00083-1

Lin, C. Y., & Lay, C. H. (2004b). Effects of carbonate and phosphate concentrations on hydrogen production using anaerobic sewage sludge microflora. International Journal of Hydrogen Energy, 29(3), 275-281. doi:10.1016/j.ijhydene.2003.07.002

Lin, C., & Lay, C. (2005). A nutrient formulation for fermentative hydrogen production using anaerobic sewage sludge microflora. International Journal of Hydrogen Energy, 30(3), 285-292. doi:10.1016/j. ijhydene.2004.03.002

Lin, Y. B., Chen, H., & Yue, L. R. (2011). Effects of K2 HPO4 on fermentative biohydrogen production of biohydrogen bacterium R3 Sp.nov. Advanced Materials Research, 280, 1-4. doi:10.4028/www.scientific.net/amr.280.1

Mandal, B., Nath, K., & Das, D. (2006). Improvement of biohydrogen production under decreased partial pressure of H2 by Enterobacter cloacae. Biotechnology Letters, 28(11), 831-835. doi:10.1007/s10529006-9008-8

Mohd Yasin, N. H., Fukuzaki, M., Maeda, T., Miyazaki, T., Hakiman Che Maail, C. M., Ariffin, H., & Wood,

T. K. (2013). Biohydrogen production from oil palm frond juice and sewage sludge by a metabolically engineered Escherichia coli strain. International Journal of Hydrogen Energy, 38(25), 10277-10283. doi:10.1016/j.ijhydene.2013.06.065

Mohd Yasin, N. H., Rahman, N. A. A., Man, H. C., Mohd Yusoff, M. Z., & Hassan, M. A. (2011). Microbial characterization of hydrogen-producing bacteria in fermented food waste at different pH values. International Journal of Hydrogen Energy, 36(16), 9571-9580. doi:10.1016/j.ijhydene.2011.05.048 Mokhtar, M., Mohd Yusoff, M. Z., Mohamad Ali, M. S., Mustapha, N. A., Wood, T. K., & Maeda, T. (2019). Pseudogene YdfW in Escherichia Coli decreases hydrogen production through nitrate

respiration pathways. International Journal of Hydrogen Energy, 44(31), 16212-16223.

doi:10.1016/j.ijhydene.2019.04.228 Morimoto, K., Kimura, T., Sakka, K., & Ohmiya, K. (2005). Overexpression of a hydrogenase gene in Clostridium paraputrificum to enhance hydrogen gas production. FEMS Microbiology Letters, 246(2), 229-234. doi:10.1016/j.femsle.2005.04.014

Mumtaz, T., Abd-Aziz, S., Rahman, A. A., Yee, P. L., & Hassan, M. A. (2008). Pilot-scale recovery of low molecular weight organic acids from anaerobically treated palm oil mill effluent (POME) with energy integrated system. African Journal of Biotechnology, 7, 3900-3905. doi:10.5897/AJB08.640

Najafpour, G. D., Shahavi, M. H., & Neshat, S. A. (2015). Assessment of biological hydrogen production processes: A review. In International Conference on Chemical and Bioprocess Engineering (pp. 1-10). Kota Kinabalu, Malaysia. doi:10.3303/CET1865042

O-thong, S., Mamimin, C., & Prasertsan, P. (2011). Effect of temperature and initial pH on biohydrogen production from palm oil mill effluent: Long-term evaluation and microbial community analysis. Electronic Journal of Biotechnology, 14(5), 1-12. doi:10.2225/vol14-issue5-fulltext-9

O-Thong, S., Prasertsan, P., Intrasungkha, N., Dhamwichukorn, S., & Birkeland, N. K. (2007). Improvement of biohydrogen production and treatment efficiency on palm oil mill effluent with nutrient supplementation at thermophilic condition using an anaerobic sequencing batch reactor. Enzyme and Microbial Technology, 41(5), 583-590. doi:10.1016/j.enzmictec.2007.05.002

Prasertsan, P., O-Thong, S., & Birkeland, N. K. (2009). Optimization and microbial community analysis for production of biohydrogen from palm oil mill effluent by thermophilic fermentative process. International Journal of Hydrogen Energy, 34(17), 7448-7459. doi:10.1016/j.ijhydene.2009.04.075 Rani, K. S., & Seenayya, G. (1999). High ethanol tolerance of new isolates of Clostridium thermocellum strains SS21 and SS22. World Journal of Microbiology and Biotechnology, 15(2), 173-178. doi:10.1023/A:1008863410460

Rasdi, Z., Nor`Aini, A. R., Abd-Aziz, S., Phang, L.-Y., Mohd Yusoff, M. Z., Chong, M. L., & Hassan, M. A. (2009). Statistical optimization of biohydrogen production from palm oil mill effluent by natural microflora. The Open Biotechnology Journal, 3(1), 79-86. doi:10.2174/1874070700903010079

Saady, N. M. C. (2013). Homoacetogenesis during hydrogen production by mixed cultures dark fermentation: Unresolved challenge. International Journal of Hydrogen Energy, 38(30), 13172-13191. doi:10.1016/j. ijhydene.2013.07.122

Sanchez-Torres, V., Mohd Yusoff, M. Z., Nakano, C., Maeda, T., Ogawa, H. I., & Wood, T. K. (2013). Influence of Escherichia coli hydrogenases on hydrogen fermentation from glycerol. International Journal of Hydrogen Energy, 38(10), 3905-3912. doi:10.1016/j.ijhydene.2013.01.031

Singh, R. P., Ibrahim, M. H., Esa, N., & Iliyana, M. S. (2010). Composting of waste from palm oil mill: A sustainable waste management practice. Reviews in Environmental Science and Bio/Technology, 9(4), 331-344. doi:10.1007/s11157-010-9199-2

Taifor, A. F., Zakaria, M. R., Mohd Yusoff, M. Z., Toshinari, M., Hassan, M. A., & Shirai, Y. (2017).

Elucidating substrate utilization in biohydrogen production from palm oil mill effluent by Escherichia coli. International Journal of Hydrogen Energy, 42(9), 5812-5819. doi:10.1016/j.ijhydene.2016.11.188 US Department of Energy (2020). Clean cities alternative fuel price report. Retrieved October 5, 2020, from https://afdc.energy.gov/fuels/prices.html

Van Ginkel, S., & Logan, B. E. (2005). Inhibition of biohydrogen production by undissociated acetic and butyric acids. Environmental Science & Technology, 39(23), 9351-9356. doi:10.1021/es0510515

Vignais, P., Magnin, J., & Willison, J. (2006). Increasing biohydrogen production by metabolic engineering. International Journal of Hydrogen Energy, 31(11), 1478-1483. doi:10.1016/j.ijhydene.2006.06.013

Vignais, P. M., & Billoud, B. (2007). Occurrence, classification, and biological function of hydrogenases: An overview. Chemical Reviews 107(10), 4206-4272. doi:10.1021/cr050196r

Xu, Q., Singh, A., & Himmel, M. E. (2009). Perspectives and new directions for the production of bioethanol using consolidated bioprocessing of lignocellulose. Current Opinion in Biotechnology, 20(3), 364-371. doi:10.1016/j.copbio.2009.05.006

Yang, H., & Shen, J. (2006). Effect of ferrous iron concentration on anaerobic bio-hydrogen production from soluble starch. International Journal of Hydrogen Energy, 31(15), 2137-2146. doi:10.1016/j. ijhydene.2006.02.009

Yossan, S., O-Thong, S., & Prasertsan, P. (2012). Effect of initial pH, nutrients and temperature on hydrogen production from palm oil mill effluent using thermotolerant consortia and corresponding microbial communities. International Journal of Hydrogen Energy, 37(18), 13806-13814. doi:10.1016/j.ijhydene.2012.03.151

Yusoff, M. Z. M., Hassan, M. A., Abd-Aziz, S., & Nor Aini, A. R. (2009). Start-up of biohydrogen production from palm oil mill effluent under non-sterile condition in 50 L continuous stirred tank reactor. International Journal of Agricultural Research, 4(4), 163-168. doi:10.3923/ijar.2009.163.168

Nutritional Characteristics of Biochar from Pineapple Leaf Residue and Sago Waste

Norshidawatie Bohari1,2, Hasmah Mohidin1,2*, Juferi Idris3,4, Yoshito Andou5, Sulaiman Man1,2, Hushairy Saidan3 and Suraiya Mahdian1,6

1Faculty of Plantation and Agrotechnology, Universiti Teknologi MARA (UiTM), Melaka Branch, Jasin Campus, 77300 Merlimau, Melaka, Malaysia 2Faculty of Plantation and Agrotechnology, Universiti Teknologi MARA (UiTM), Sarawak Branch, Samarahan Campus, 94300 Kota Samarahan, Sarawak, Malaysia 3Faculty of Chemical Engineering, Universiti Teknologi MARA (UiTM), Sarawak Branch, Samarahan Campus, 94300 Kota Samarahan, Sarawak, Malaysia 4Faculty of Chemical Engineering, Universiti Teknologi MARA (UiTM), 40450 Shah Alam, Selangor, Malaysia

5Graduate School of Life Science and System Engineering, Kyushu Institute of Technology, Kitakyushu, Fukuoka, Japan

6Faculty of Plantation and Agrotechnology, Universiti Teknologi MARA (UiTM), Sarawak Branch, Mukah Campus, 77300 Mukah, Sarawak, Malaysia

ABSTRACT

Biochar produced from biomass with high nutrient content is essential for improving the quality of agricultural soils. An abundance of biomass is converted into biochar with high nutrient content, but studies on the conversion of pineapple and sago waste into biochar are still limited. This research aimed to produce biochar from pineapple leaf (PLB), sago bark (SBB), and sago pith (SPB) through the carbonization process with low temperature. The samples were carbonized using a laboratory electric oven at a low temperature of 350°C. The raw biomass and biochar produced were then subjected to elemental analysis and characterization. The mineral contents of carbonized biochar such as K, N, S, Mg, and Ca increased from those of the feedstock concentrations. For PLP, K element increased 24-fold from $2.44 \pm 0.73\%$ to $48.32 \pm 9.92\%$, while N element increased from $6.13 \pm 2.39\%$ to $8.33 \pm 5.34\%$. However, for both SBB and SPB, N and K nutrients increased by 2-fold. The study reveals that pineapple leaf biochar has the potentials to be used as an alternative soil amendment to elevate soil nutrient and quality.

Keywords: Biochar, low carbonization, pineapple leaf, sago bark, sago pith residue

INTRODUCTION

With the growing in agriculture sector, the amount of agro-waste generated annually has also been increasing. Agamuthu (2009) stated that about 998 million tons of crop residues, including biomass wastes and crop fibre residues, were produced yearly, and Asia is the main contributor. Malaysia recorded more than 70 million tons of crop residues annually (Chong et al., 2014). Agricultural wastes fibers such as sago wastes and pineapple residues have contributed to a massive landfill problem and solid pollutants to the environment after harvesting. In Sarawak, sago palm (Metroxylon sagu. Rottb.) is

a new emerging plantation crop, with about 43,326 hectares of sago crop are grown in large scale in Mukah (Naim et al., 2016). Their findings indicated that the highest contributor of sago wastes were residues from sago pith residues (SPW) and sago bark wastes (SBW). According to another study conducted by Chong et al. (2014), approximately 90% of the sago starch is produced in Sarawak, and sago bark is an abundant waste product from sago starch extraction. Pineapple (Ananas comosus) is a highly nutritive, non-seasonal tropic fruit with a fine f lavor. In Malaysia, pineapple is the top five fruits with the most promising demand in the local and export markets (Nazri & Pebrian, 2017). In Sarawak, pineapple production has increased by 70% from 17 metric tonnes per hectare in 2014 to 29 metric tonnes per hectare (Edward, 2016). Sarawak is targeting 2,500 hectares by 2020, with an average production of 45 metric tons per hectare. Pineapple leaf fibre (PLF) is one of the abundantly available waste materials in Malaysia and has not been studied as required. According to Asim et al. (2015), PLF is one of the waste materials in the agriculture sector, which is widely grown in Malaysia as well as Asia. Commercially pineapple fruits are very important and leaves are considered as organic waste materials that are left behind after fruit harvesting, which is being used for producing natural fibres. The chemical composition of PLF constitutes holocellulose (70%–82%), lignin (5%–12%), and ash (1.1%). In Malaysia, waste management of these leaves is improving time to time, whereby the leaves are collected and consigned for research and industry utilization (Padzil et al., 2020). Pineapple residues can be categorized as a contributor to wastes because they consist of pulp, peels, stem, and leaves (Nunes et al., 2009). If these crop residues are not handled with proper disposal, it may result in bad environmental effect where the residues might inhibit the drainage system after disposal. In addition, the cost of disposal is expensive due to high transportation cost and restricted landfill for disposal activity (Upadhyay et al., 2010).

Biochar is a carbon-rich product produced from the slow thermochemical pyrolysis of biomass materials from organic wastes such as crop residues, livestock manure, sewage sludge, and composts and then applied to soils as an amendment. Interest in biochars has recently been driven by two major global issues: climate change and the realization of the need for sustainable soil management. Biochar can be described as carbonized product after pyrolysis process which can be obtained from residues or plant biomass which highly improves soil properties and increases crop growth and soil fertility. Fu et al. (2016) indicated that the increase of pyrolysis temperature increased pH, electrical conductivity (EC), and carbon (C) content of pineapple biochar. This proves that biochar has the potential as an additive agent to increase nutrient content and enhance its properties. Lehmann (2007) stated that all organic material added to the soil would give significant effect in increasing soil functions variety, including retention (ability to reserve nutrients) for plant growth. However, biochar holds nutrients more effectively, so there are more available nutrients compared to leaf, compost, and manure fertilizer. Biochar application into soil has the potential of increasing the C content, water and nutrient retention in

soil (Mawardiana et al., 2013).

Due to high cellulose and lignin contents in sago bark and pineapple waste but with low commercial values, their disposal is a problem to the mills due to their large quantity. However, a few research work has been done on the conversion of these underutilized agrowastes such as pineapple waste and sago waste into biochar as an alternative soil amendment. Thus, the aim of this study is to evaluate the potential of nutrients produced by biochar from pineapple leaf, sago bark and sago pith as organic feedstocks under controlled carbonization to elevate soil nutritional status and soil quality.

MATERIALS AND METHODS

Sample Preparation

Raw PL biomass was obtained from pineapple smallholders in Kampung Melayu, Samarahan meanwhile SB and SP biomass were purchased from Sago Mill in Mukah, Sarawak. The raw biomass was washed and oven dried at 105°C until constant weight. Then it was crushed into fine powder and ground into a size of about 2 mm using a heavyduty grinder (Claoston et al., 2014).

Carbonization Preparation

Biochar production was performed according to Leng et al. (2011). Samples were placed into ceramic crucibles with fitting lids and carbonized at 350°C for 2 h in a large chamber muffle furnace (Type 62700; Thermo Scientific Barnstead/Thermolyne, USA). All biochars were then ground to pass a 1-mm sieve and kept at room temperature prior to analysis. The yield of biochar was calculated as follows:

Biochar yield (%) =
$$\frac{Mass\ of\ biochar\ (g)}{Mass\ of\ raw\ material\ after\ oven\ dry\ (g)} \times 100\%$$

Analytical Methods

Elemental analysis was carried out based on Idris et al. (2014). The main elements obtained from raw PL, SB and SP biomass, and PL, SB, and SP biochar samples were analyzed using an inductive coupled plasma—optical effluent spectrophotometer (ICP—AES, model: Perkin Elmer 2100). Approximately 1–2 g of sample was first placed in the furnace and the temperature was gradually increased to 300°C until smoke ceased and was subsequently raised to 500°C. The process continued at this temperature until white or greyish-white ash was obtained. The sample was then digested using concentrated hydrochloric acid (37% v/v) and nitric acid (20% v/v). pH analysis was measured using an Oakton pH 700 Benchtop Meter (Barwant et al., 2018). For Electrical Conductivity (EC) measurement, the samples was soaked with deionized water. The ratio used was 1:5 of solid/water and agitated for 24 h. The EC was measured and recorded using a CON 700 EC meter (Eutech USA). For the FTIR (Fourier-transform Infrared Spectroscopy) analyses, 10 mg of biochar was mixed with 190 mg of spectroscopic-grade KBr; the

mixture was first hand ground and then ground in a Wig-L-bug using a stainless steel vial with a stainless steel ball pestle for 30 s. The FTIR measurements were performed with an ATR-ThermoFisher Nicolet iS5 FTIR spectrometer. The scans were carried out in the range from 4000 to 650 cm $^{-1}$ with a resolution of 4 cm $^{-1}$ and 64 scans per sample. Thermogravimetric analysis (TGA) was performed using a thermogravimetric analyzer (Mettler Toledo) under air atmosphere at a heating rate of 10° C/min from ambient temperature to 600° C. A sample mass of 3.5 ± 0.5 mg was used for each analysis and the mean values were used provided that the deviations were within 5 %. The mass loss (TG) of the samples was represented as a function of temperature. Surface morphologies of raw and biochar of SB, SP, and PL were identified by SEM (JCM-6000, JEOL, Japan). The samples were prepared by coating with carbon at the outer layer of the sample, and then elemental components were under microscopy detection. X-ray diffraction (WAXD) analysis was performed using an X-ray diffractometer (MiniFlex 600, Rigaku Co., Japan) at 40 kV and 15 mA at room temperature. The X-ray initiator used was Cu K α radiation ($\lambda = 1.54$ angle was examined from 5° to 60° at a rate of 10° /min.

RESULTS AND DISCUSSION

Characteristic of Biomass

The results for the elemental analysis of pineapple leaf, sago bark, and sago pith for raw biomass are shown in Table 1. The basic elements, namely, primary macronutrients (N, P, and K) and the secondary micronutrients (Ca, Mg, and S) of the raw incinerated pineapple leaves were adequate and can support the initiation of any plant growth.

Table 1
Elemental compositions of raw biomass

| Element | Composition (%) | | | | |
|--------------|-----------------|------------------|-------------------|--|--|
| Element - | Pineapple leaf | Sago bark | Sago pith residue | | |
| C | 48.4 ± 0.27 | 49.73 ± 5.31 | 49.67 ± 6.58 | | |
| \mathbf{N} | 6.13 ± 2.39 | 4.43 ± 3.65 | 3.38 ± 1.62 | | |
| O | 41.77 ± 2.29 | 41.96 ± 6.19 | 45.92 ± 7.63 | | |
| Mg | 0.56 ± 0.18 | 0.23 ± 0.23 | 0.24 ± 0.13 | | |
| P | 0.44 ± 0.22 | 0.11 ± 0.24 | 0.14 ± 0.08 | | |
| S | 0.14 ± 0.03 | 0.24 ± 0.11 | 0.03 ± 0.04 | | |
| K | 2.44 ± 0.73 | 2.27 ± 1.21 | 0.20 ± 0.16 | | |
| Ca | 0.12 ± 0.14 | 1.03 ± 0.23 | 0.42 ± 0.28 | | |

N no of repetition 30

It was observed that the raw PL and SB had high K content compared to SP. This result might be due to the naturally high K in pineapple leaves.

Pineapple waste is one type of organic material containing a high C/N ratio (50%–70%). Materials that

have high C/N give a greater influence to change the soil physical properties (Ridwan et al., 2018). According to Hunt et al. (2010), by converting biomass into biochar, many of its carbon content would become fixed into a more stable form. The exothermic process during the biochar production via pyrolysis precipitated carbon dioxide onto the biochar surfaces (Lehmann, 2007).

Comparing the results in Tables 1 and 2, for PLP, K element increased of 24-fold from $2.44 \pm 0.73\%$ to $48.32 \pm 9.92\%$, while N element increased from $6.13 \pm 2.39\%$ to $8.33 \pm 5.34\%$. However, for both SBB and SPB, N and K elements increased 2-fold. The highest yield of biochar was 52.00% (SBB), followed by 51.43% (PLB), and 46.48% (SPB). After carbonization at 350° C, the differences in yield between all of them were small and insignificant comparatively. This indicates that although with low energy consumption through the oven-drying electrical source, the overall yield values were still acceptable. It was observed that the C content in SBB and SPB increased but otherwise for PLB (Table 2) after carbonization. As pyrolysis occurred, the oxygen content of all the biomass decreased. However, the elements of K, Mg, and S increased in PLB and SPB compared to those in SBB. Due to the carbonization at 350° C, the weight loss and volatile content disappeared. Hence, the nutrient content in biochar accumulated and increased after carbonization. This result is supported by Idris et al. (2014) where the utilization of biochar improved the soil fertility and reduced the use of chemical fertilizers compared

Table 2
Characteristic of elemental composition on biochar

| Properties | Pineapple leaf | Sago bark | Sago pith residue |
|---------------------------|------------------|------------------|-------------------|
| Yield (%) | 51.43 | 52.00 | 46.48 |
| рН | 8.78 | 8.59 | 7.93 |
| EC (mS cm ⁻¹) | 7.38 | 5.43 | 4.26 |
| Elemental analysis | | Composition (%) | |
| С | 19.37 ± 2.03 | 51.36 ± 3.58 | 61.66 ± 9.17 |
| N | 8.33 ± 5.34 | 10.65 ± 2.07 | 6.18 ± 5.41 |
| O | 21.95 ± 5.92 | 33.24 ± 0.63 | 28.06 ± 7.83 |
| Mg | 1.27 ± 0.93 | 0.16 ± 0.15 | 0.40 ± 0.29 |
| P | 0.39 ± 0.05 | 0.07 ± 0.07 | 0.18 ± 0.17 |
| S | 0.32 ± 0.14 | 0.07 ± 0.09 | 0.05 ± 0.06 |
| K | 48.32 ± 9.92 | 4.01 ± 3.22 | 0.48 ± 0.11 |
| Ca | 0.05 ± 6.33 | 0.44 ± 0.19 | 2.99 ± 1.68 |

to raw biomass for the same purpose with high mineral and low heavy metal contents. In addition, biochar from biomass can be used to prevent erosion and maintain soil moisture while reducing pollution to the environment (Lim & Zaharah, 2000).

Generally, PLB, SBB, and SPB show high pH values. The pH of pineapple leaf biochar was slightly higher (>8) compared to sago bark and sago pith residue biochar (Table 2). The high pH indicates that biochars are good soil liming materials. This finding is in agreement with that of Leng et al. (2017). The property of EC indicates a slightly higher salinity in PLB compared to those in SBB and SPB. Furthermore, higher mineral ash in biochar probably has higher electrical conductivity especially those that have high K+ ion content as in PLB, due to the mobility of the K+ ions (Joseph et al., 2007). As PL

biochar is rich in minerals, it may be better suited as an alternative organic fertilizer and can acts as a potential soil amendment. Interestingly, among the macronutrients presence, the K content in PL biochar increased tremendously by 20-fold while the K contents in SB and SP biochar increased only 2-fold. High concentrations of potassium (K) and nitrogen (N) could probably be due to the usage of fertilizers which contain potassium nitrate (KNO3)

in the commercial pineapple cultivation. Meanwhile, sago palm is mainly in its natural state condition and often left unfertilized in the mangrove swamp areas. However, there is no clear pattern for the P element in this study. Besides, the concentration of nutrients in the biochar also depends on the process of partial defractionation and/or devolatilization of these nutrients at elevated temperatures (Claoston et al., 2014; Hossain et al., 2011).

Fourier Transform Infrared Spectroscopy (FTIR)

Two weak peaks were observed at 2840–3000 cm–1 for PLB due to the C–H stretching from aliphatic groups (Figure 1). The C–H stretching of SBB and SPB between 2840–3000 cm–1 reveals the existence of alkane groups and this finding is supported by the findings by Claoston et al. (2014) (Figures 2 and 3). The stretching vibration of the C=C group (1566–1650 cm–1) was identified in the spectrum of PLB which shows the existence of cyclic alkene.

The existence of conjugated aldehyde in SBB and SPB was observed where the peak showed the C=O stretching (1685–1710 cm-1). According to the FTIR spectra analysis, all the biochars exhibited the existence of the C-H stretching, aromatic C=C stretching, and C=O stretching. This observation indicates that biochar began to carbonize as the temperature increased during carbonization, which suggests degradation and depolymerization of cellulose, hemicelluloses and lignin (Cantrell et al., 2012). Table 3 shows the vibration characteristics and compound class for each wavenumber. Overall, based on the FTIR spectra for biochar, carbonization at lower temperatures resulted in dehydration, beginning of bond breakage, and transformational products (Cantrell et al., 2012).

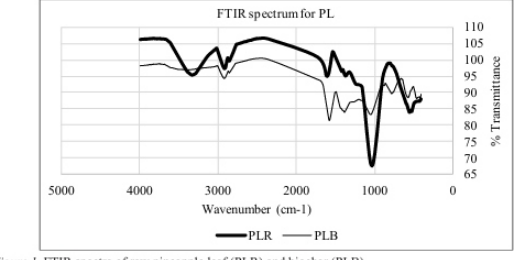


Figure 1. FTIR spectra of raw pineapple leaf (PLR) and biochar (PLB)

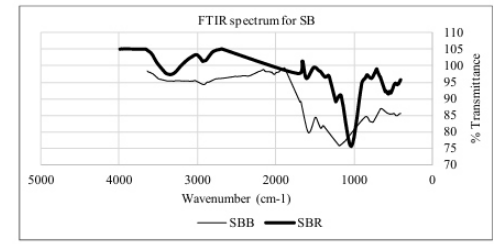


Figure 2. FTIR spectra of raw sago bark (SBR) and biochar (SBB)

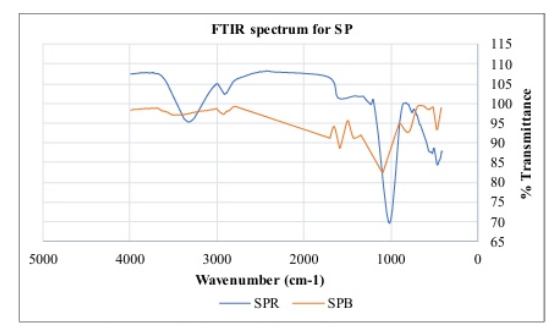


Figure 3. FTIR spectra of raw sago pith (SPR) and biochar (SPB)

Table 3

FTIR spectra of pineapple leaves and sago waste biochar

| Wavenumber (cm ⁻¹) | Pineapple leaf | Sago bark | Sago pith | Vibration characteristics | Compound class |
|-----------------------------------|-------------------|--------------|--------------|---------------------------|---------------------|
| 3000-2840 | + | + | + | C-H stretching | Alkane |
| 1710-1685 | 2 | + | + | C=O stretching | Conjugated aldehyde |
| 1650-1566 | + | - | - | C=C stretching | Cyclic alkene |
| 1450-1390 | - | + | + | C-H bending | Methyl group |
| 1385-1380 | + | - | - | C-H bending | Gem dimethyl |
| 1250-1020 | + | - | 1 | C-N stretching | Amine |
| 1205-1124 | - | + | - | C-O stretching | Tertiary alcohol |
| 1124-1087 | - | - | + | C-O stretching | Secondary alcohol |
| | | | | | |

In this analysis, all biochar samples showed a similar thermal degradation where SPB was clearly degraded below PLB and SBB. At 10% degradation, each sample degraded at different temperatures of 374.10, 378.27, and 364.10°C for PLB, SBB, and SPP, respectively (Figure 4). The result shows that SPB was easily degraded due to its characteristics where the samples lost its proportion with the increasing degradation temperature.

Scanning Electron Microscopy/Energy Dispersive X-Ray Analyzer (SEM/EDX)

The result shows that the SEM images have a large amount of pores. The pore structure of PLR was well defined and smaller compared to that of PLB (Figure 5). After carbonization, the biochar produced was observed to have large pores size exposing a variety of pore shapes and became cracked. The structure seemed to be fragile due to its thin walls and

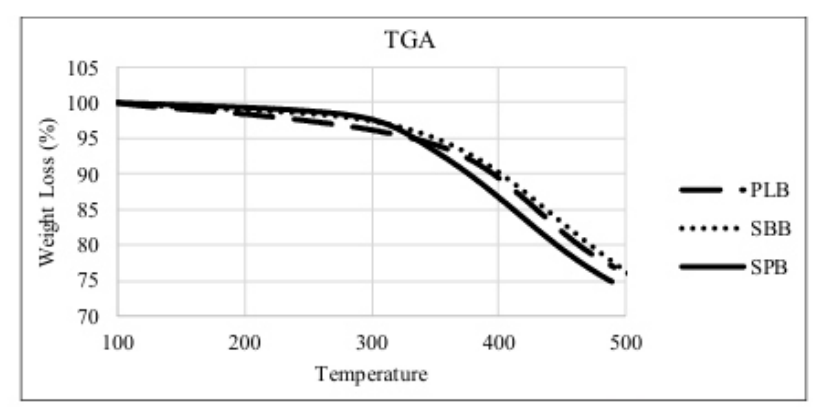
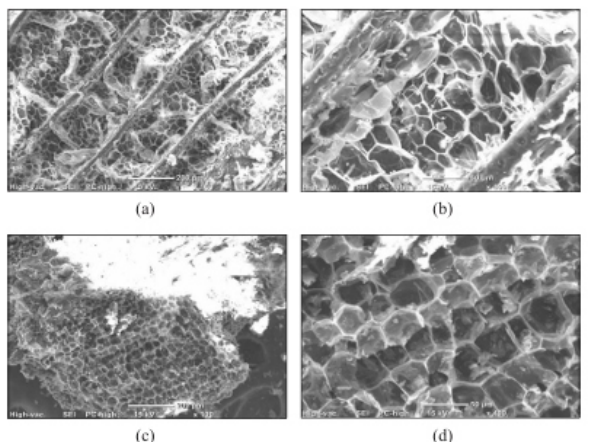


Figure 4. Thermal analysis of the biochars obtained from pineapple leaf (PLB), sago bark (SBB), and sago pith (SPB)

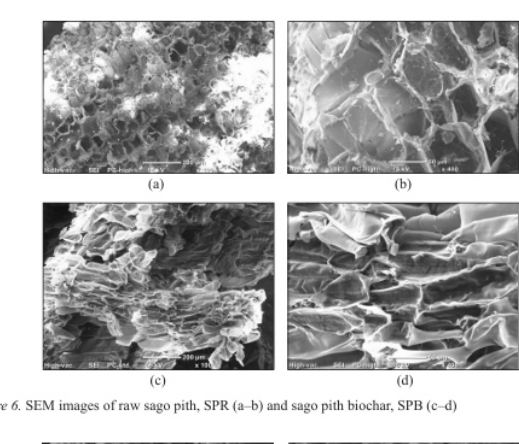
easily broke during pyrolysis. The surface of SBR was rough with smaller pores. After carbonization, many well-defined and softened pores were produced with large pores structure (Figure 6). This might

be caused by the evolution of volatile organic compounds. Wahi et al. (2015) stated that devolatilization during pyrolysis might contribute to low denseness, improved pores formation of biochar, and higher porosities. In general, the increase in surface area at a high pyrolysis temperature is due to the removal of volatile material resulting in increased micropore volume (Ahmad et al., 2012). Based on the outer appearance of SPR (Figure 7), the surface was smooth with many pores. After pyrolysis, biochar produced was observed to have a large pore size. This



(c) (d) Figure 5. SEM images of raw pineapple leaf, PLR (a–b) and pineapple leaf biochar, PLB (c–d)

indicates that the pyrolysis process was fully utilized to form porous structure of biochar (Claoston et al., 2014). Zakaria et al. (2019) stated that the pores produced could be due to the degradation of organic materials.



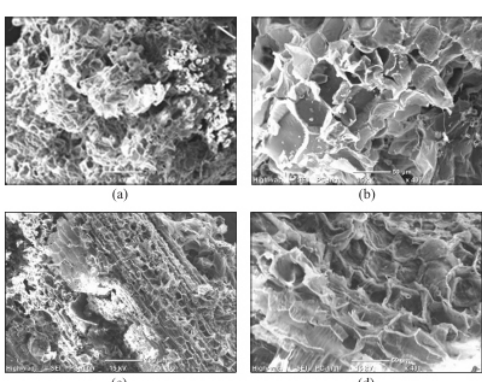


Figure 7. SEM image of raw sago pith, SPR (a-b) and sago pith biochar, SPB (c-d)

X-Ray Diffraction (XRD)

The XRD shape of raw material is demonstrated in Figure 8. The diffractograms of SBR and PLR showed one reflection, corresponding to 2θ values of 22.06° and 22.28° , respectively. Meanwhile, SPR showed two reflections, corresponding to 2θ values of 17.52° and 22.52° . The narrower peaks of raw indicate the presence of cellulose structure (Shaaban et al., 2013).

Decreasing peaks at 20 values of 21.92°, 21.32°, and 21.54° were observed for SBB, SPB, and PLB, respectively (refer to Figure 9). It might be due to the decomposition of cellulose element. According to Shaaban et al. (2013), the increasing temperature during pyrolysis may cause the peaks of stipulated angles disappear, and cellulose starts to decompose.

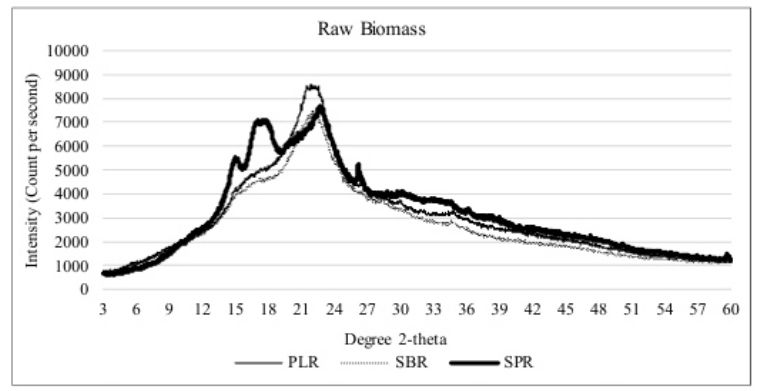


Figure 8. XRD patterns of raw pineapple leaf (PLR), sago bark (SBR), and sago pith (SPR)

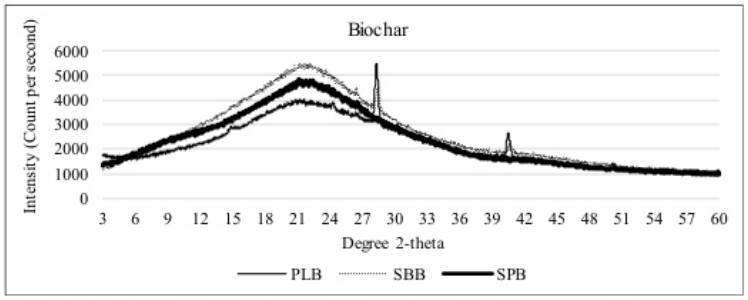


Figure 9. XRD patterns of pineapple leaf (PLB), sago bark (SBB), and sago pith (SPB) biochar

The elemental analysis showed the highest nutrient content in PLB compared to SBB and SPB. PLB has the highest nutrient content of Mg, S, and K. SEM micrographs indicate the best development of pores in PLB compared to those in SBB and SPB, and the results are comparable with other studies. The plant growth in terms of root growth and photosynthesis capacity requires high macronutrients. It can be concluded that the pineapple leaf biochar can be the most suitable additive to be applied to the soil to elevate soil nutritional status and quality.

CONCLUSION

The production of biochar from underutilized pineapple leaf and sago waste was successfully determined using simple carbonization at low temperature. This study showed all minerals (i.e., P, K, Mg, Ca) increased from their initial concentrations in the feedstock. The minerals contents in carbonized

biochar such as K, N, S, Mg, and Ca also increased. For PLP, K element increased 24-fold from $2.44 \pm 0.73\%$ to $48.32 \pm 9.92\%$, while N element increased from $6.13 \pm 2.39\%$ to $8.33 \pm 5.34\%$. However, for SBB and SPB, N and K nutrients only increased 2-fold. SEM micrographs indicate the best development of pores in PLB compared to those in SBB and SPB, and the results are comparable with other studies. The overall results on biochar obtained from pineapple leaves, sago bark, and sago pith residues, indicate the potential of inherent nutrient content in PLB, SBB and SPB to be used as an alternative soil amendment. However, future work needs to be done to quantify the essential nutrients generated to make further recommendations. This study showed that the underutilized pineapple leaf biochar could potentially be used as an alternative to elevate soil nutritional status and to mitigate environmental problems.

ACKNOWLEDGEMENT

The authors are grateful to Universiti Teknologi MARA, Malaysia, UiTM Sarawak Branch, Samarahan Campus, UiTM Melaka Branch, Jasin Campus, and Kyushu Institute of Technology, Japan for the financial and technical support in this study.

REFERENCES

Agamuthu, P., (2009). Challenges and opportunities in agro-waste management: An Asian perspective. R e t r i e v e d S e p t e m b e r 2 0 , 2 0 1 8 , f r o m http://www.env.go.jp/recycle/3r/en/forum asia/results/pdf/20091111/08.pdf

Ahmad, M., Lee, S. S., Dou, X., Mohan, D., Sung, J. K., Yang, J. E., & Ok, Y. S. (2012). Effects of pyrolysis temperature on soybean stover-and peanut shell-derived biochar properties and TCE adsorption in water. Bioresource Technology, 118, 536-544. doi:10.1016/j.biortech.2012.05.042

Asim, M., Abdan, K., Jawaid, M., Nasir, M., Dashtizadeh, Z., Ishak, M. R., & Hoque, M. E. (2015). A review on pineapple leaves fibre and its composites. International Journal of Polymer Science, 2015 1–16. doi:10.1155/2015/950567

Cantrell, K. B., Hunt, P. G., Uchimiya, M., Novak, J. M., & Ro, K. S. (2012). Impact of pyrolysis temperature and manure source on physicochemical characteristics of biochar. Bioresource Technology, 107, 419–428. doi:10.1016/j.biortech.2011.11.084

Chong, K. H., Law, P. L., Rigit, A. R. H., Baini, R., & Shanti, F. S. (2014). Sago bark as renewable energy. Journal of Civil Engineering, Science and Technology, 5(2), 29-34. doi:10.33736/jcest.136.2014

Claoston, N., Samsuri, A. W., Ahmad Husni, M. H., & Mohd Amran, M. S., (2014). Effects of pyrolysis temperature on physicochemical properties of empty fruit bunch and rice husk biochars. Waste Management and Research, 32(4), 331-339. doi:10.1177/0734242x14525822

Edward, C. (2016, August 14). Pineapple planters all excited about MD2. Borneo Post. Retrieved June

- 23, 2020, from https://www.theborneopost.com/2016/08/14/pineapple-planters-all-excited-about-md2/
- Fu, B., Ge, C, Yue, L., Luo, J., Feng, D., Deng, H., & Yu, H. (2016). Characterization of biochar derived from pineapple peel waste and its application for sorption of oxytetracycline from aqueous solution. BioResources, 11(4), 9017–9035. doi:10.15376/biores.11.4.9017-9035
- Hossain, M. K., Strezov, V., Chan, K. Y., Ziolkowski, A., & Nelson, P. F. (2011). Influence of pyrolysis temperature on production and nutrient properties of wastewater sludge biochar. Journal of Environmental Management, 92(1), 223–228. doi:10.1016/j.jenvman.2010.09.008
- Hunt, J., DuPonte, M., Sato, D., & Kawabata, A. (2010). The basics of biochar: A natural soil amendment. Soil and Crop Management (SCM-30). Retrieved September 20, 2018, from http://www.ctahr.hawaii.edu/oc/freepubs/pdf/SCM-30.pdf
- Idris, J., Shirai, Y., Ando, Y., Ali, A. A. M., Othman, M. R., Ibrahim, I., & Hassan, M. A. (2014). Production of biochar with high mineral content from oil palm biomass. Malaysian Journal of Analytical Sciences, 18(3), 700–704.
- Joseph, S. D., Downie, A., Munroe, P., Crosky, A., & Lehmann, J. (2007, December 9-11). Biochar for carbon sequestration, reduction of greenhouse gas emissions and enhancement of soil fertility; A review of the materials science. In Proceedings of the Australian combustion symposium (pp. 130-133). Sydney, Australia. Lehmann, J. (2007). Bio-energy in the black. Frontiers in Ecology and the Environment, 5(7), 381–387. doi:10.1890/1540-9295(2007)5[381:bitb]2.0.co;2
- Leng, L. Y., Husni, M. H. A., & Samsuri, A. W., (2011). Comparison of the carbon-sequestering abilities of pineapple leaf residue chars produced by controlled combustion and by field burning. Bioresource Technology, 102(22), 10759–10762. doi:10.1016/j.biortech.2011.08.131
- Lim, K. C., & Zaharah, A. R. (2000). Decomposition and N & K release by oil palm empty fruit bunches applied under mature palms. Journal of Oil Palm Research, 12(2), 55–62.
- Mawardiana, Sufardi., & Husen E. (2013). Pengaruh residu biochar dan pemupukan NPK terhadap sifat kimia tanah dan pertumbuhan serta hasil tanaman padi (Oryza sativa L.) musim tanam ketiga [Residual effect of biochar and NPK fertilization toward the dynamics of nitrogen, soil chemical properties and rice crop in third season planting]. Jurnal Manajemen Sumber Dayalahan, 2(3), 255–260.
- Naim, H. M., Yaakub, A. N., & Hamdan, D. A. A. (2016). Commercialization of sago through estate plantation scheme in Sarawak: The way forward. International Journal of Agronomy, 2016, 1–6. doi:10.1155/2016/8319542
- Nazri, A. M., & Pebrian, D. E. (2017). Analysis of energy consumption in pineapple cultivation in Malaysia: A case study. Pertanika Journal of Science & Technology, 25(1), 17–28.
- Nunes, M. C. N., Emond, J. P., Rauth, M., Dea, S., & Chau, K. V., (2009). Environmental conditions

encountered during typical consumer retail display affect fruit and vegetable quality and waste. Postharvest Biology and Technology, 51(2), 232–241. doi:.1016/j.postharvbio.2008.07.016

Padzil, F. N. M., Ainun, Z. M. A., Kassim, N. A., Lee, S. H., Lee, C. H., Ariffin, H., & Zainudin, E. S. (2020). Chemical, physical and biological treatments of pineapple leaf fibres. In M. Jawaid, M. Asim, P. Tahir & M. Nasir (Eds.), Pineapple leaf fibers (pp. 73–90). Singapore: Springer

Ridwan, I., Jaya, A. M., & Mantja, K. (2018). Pengembangan bioindustri kompos limbah pertanian melalui pemberdayaan masyarakat pesisir di Kecamatan Labakkang [Development of Agricultural Waste Compost Bioindustry through Empowerment of Coastal Communities in Labakkang District]. Jurnal Dinamika Pengabdian (JDP), 3(2), 165–176. doi:10.20956/jdp.v3i2.4248

Shaaban, A., Se, S., Mitan, N. M. M., & Dimina, M. F. (2013). Characterization of biochar derived from rubber wood sawdust through slow pyrolysis on surface porosities and functional groups. Procedia Engineering, 68, 365-371. doi:10.1016/j.proeng.2013.12.193

Upadhyay, A., Lama, J. P., & Tawata, S. (2010). Utilization of pineapple waste. Journal of Food Science and Technology Nepal, 6, 10–18. doi:10.3126/jfstn.v6i0.8255

Wahi, R., Aziz, S. M. A., Hamdan, S., & Ngaini, Z. (2015, December 14-16). Biochar production from agricultural wastes via low-temperature microwave carbonization. In IEEE International RF and Microwave Conference (RFM) (pp. 244-247). Kuching, Malaysia.

Zakaria, Z. A., Boopathy, R., Dib, J. R. (2019). Valorisation of agro-industrial residues – volume I: Biological approaches. Cham, Switzerland: Springer Nature AG.

Static Mechanical, Thermal Stability, and Interfacial Properties of Superheated Steam Treated Oil Palm Biomass Reinforced Polypropylene Biocomposite

Muhammad Nazmir Mohd Warid1, Tengku Arisyah Tengku Yasim-Anuar1, Hidayah Ariffin1,2*, Mohd Ali Hassan1, Yoshito Andou3 and Yoshihito Shirai3

1Department of Bioprocess Technology, Faculty of Biotechnology and Biomolecular Sciences, 43400 UPM Serdang, Selangor, Malaysia

2Laboratory of Biopolymer and Derivatives (BADs), Institute of Tropical Forestry and Forest Products (INTROP), Universiti Putra Malaysia, 43400 UPM Serdang, Selangor, Malaysia

3Department of Biological Functions and Engineering, Graduate School of Life Science and System Engineering, Kyushu Institute of Technology, 2-4 Hibikino, Wakamatsu, Fukuoka 808-0196, Japan

ABSTRACT

In this study, three types of oil palm biomass (OPB) namely, oil palm mesocarp fiber (OPMF), oil palm empty fruit bunch (OPEFB) and oil palm frond (OPF), were studied and compared as the alternative fillers in the biocomposite reinforced polypropylene (PP). The fibers were treated using the optimal condition of superheated steam treatment obtained from previous study. The OPB/PP biocomposites at weight ratio of 30:70 were fabricated by melt blending technique and hot pressed moulding. Results showed that the tensile and flexural properties of optimized-SHS-treated OPB/PP biocomposites were improved by 9-30% and 9-12%, respectively compared to the untreated OPB/PP biocomposites. The same observation was recorded for thermal stability. Improved surface morphology as shown by the tensile fracture surface indicates better interfacial adhesion between SHS treated OPB fibers with PP matrix during blending. Overall results showed that OPF/PP biocomposites had better properties compared to biocomposites prepared from OPMF and OPEFB, suggesting that OPF is a better OPB fiber choice as a filler in PP reinforced biocomposite.

Keywords: Biocomposite, oil palm mesocarp fiber (OPMF), oil palm empty fruit bunch (OPEFB), oil palm frond (OPF), superheated steam (SHS) treatment

INTRODUCTION

Recently, research on the utilization of natural fibers over the synthetic fibers as the reinforcement in biocomposite has been extensively conducted due to the advantages of natural fibers. Natural fibers have low density, high toughness, good specific strength properties, good thermal and insulation properties, low in cost, non-abrasive to the processing equipment, biodegradable and easy to recycle (Acha et al., 2007; Akil et al., 2011; Bogoeva-Gaceva et al., 2007; Raju et al., 2008; Spoljaric et al., 2009). Several natural fibers have been tested for biocomposite fabrication such as kenaf, bamboo, baggase and rice husk. Due to the large amount of oil palm biomass (OPB) in Malaysia, the utilization of OPB to produce valuable products such as biocomposites has been studied (Karuppuchamy et al., 2015; Nordin et al.,

2013; Then et al., 2013). When using natural fiber as filler in polymer composite, surface modification is commonly needed due to incompatibility with the polymer matrix. Natural fiber consists of hydroxyl (OH) group, causes it to be hydrophilic in nature, whereas polymer used in composite application is commonly hydrophobic. Such differences in wetting properties makes them difficult to achieve homogenous dispersion (Yasim-Anuar et al., 2020). Without surface modification, the resulting biocomposites may have poor mechanical properties, mainly due to poor stress transfer between both polymer matrix and fibers (Warid et al., 2016). There have been numerous methods used for surface modification of the natural fibers, including superheated steam (SHS) treatment (Nordin et al., 2013). Optimization study of SHS treatment on the oil palm biomass has been done in order to prepare suitable properties of fibers for biocomposite purpose (Warid et al., 2016). A previous study by Warid et al. (2016) revealed that SHS treatment was able to alter the fiber surface by removing hemicellulose and silica bodies, thus abled to enhance the fiber thermal stability and remove its moisture. This helps in enhancing compatibility with the polymer matrix. This study aims to compare the use of several types of oil palm biomass, OPMF, OPEFB and OPF as reinforcement material in polypropylene biocomposite. The biocomposites produced were characterized for their mechanical, thermal stability, and surface morphological properties.

MATERIALS AND METHODS

Raw Materials

OPMF and OPEFB were obtained from Seri Ulu Langat Palm Oil Mill, Selangor, Malaysia while OPF was obtained from Taman Pertanian Universiti (TPU), Universiti Putra Malaysia (UPM). OPF was first shredded and pressed to remove the juice as described by Abdullah et al. (2015). The preparation of raw OPMF, OPEFB and OPF were conducted as described by Nordin et al. (2013). The size of each fiber was about 8-10cm in length and no further mechanical treatment was done prior to SHS treatment.

Superheated Steam Treatment

OPB fibers were treated using lab scale superheated steam oven (QF-5200C, Naomoto Corporation, Osaka, Japan) under ambient pressure as described by Nordin et al. (2013). Steam flow rate and heater power of SHS oven were kept constant at maximum value, 4.95 kg/h and 6.6 kW, respectively. OPB fibers were treated using optimized SHS treatment conditions which were obtained from the previous optimization studies (Warid et al., 2016). The optimized SHS treatment temperature and retention time for each OPB fibers are shown in Table 1.

Table 1
Optimized SHS treatment temperature and retention time for OPMF, OPEFB and OPF

| Fiber | Temperature (°C) | Retention time (mins) |
|-------|------------------|-----------------------|
| OPMF | 265 | 5 |
| OPEFB | 280 | 5 |
| OPF | 300 | 9 |

Biocomposite Production

Untreated and SHS-treated OPB fibers were then subjected to grinding using Wiley-type Mill to obtain the OPB powders. OPB powders which size is less than 150 um was chosen for the biocomposite production. The PP and OPB powders were dried in an oven at 60°C prior to use. The biocomposites were prepared by melt blending PP and fibers in a Brabender internal mixer (Germany) at 170°C with 50 rpm rotor speed for 15 minutes. The weight ratio of OPB/PP was fixed at 30:70. The PP pellet was first loaded in the mixer chamber for about 2 minutes to melt. Next, OPB fibers were added into the mixing chamber and mixing was continued for another 13 minutes. These compounded materials were then compressed into 1-3 mm thickness sheets with length of 150 mm x 150 mm by a hydraulic hot-press at 170°C for 5 minutes, followed by cold pressing at 30°C for 5 minutes.

Chemical Compositional Analysis

Determination of lignin, cellulose and hemicellulose in the OPMF, OPEFB and OPF was done gravimetrically according to the method by (Iwamoto et al., 2008).

Mechanical Test Analysis

For tensile test, the test specimens were cut from 1mm sample sheets using a dumbbell shape cutter of ATM D638 standard. A crosshead speed of 5mm/min was used, and the tests were performed at 25°C. The results were expressed in terms of tensile strength, tensile modulus and elongation at break. The test was performed on five specimens for each formulation and the average values and standard deviations were reported.

For flexural test, a three-point bending test was conducted on the biocomposites according to ASTM D790 standard. The test was conducted at 25°C with a crosshead speed of 1.3 mm/min and a support span length of 48mm. The results were expressed in terms of flexural strength and flexural modulus.

Thermogravimetric Analysis

Thermogravimetric analysis (TGA) was conducted on a TG analyzer model TG4000 in order to confirm the change in the composition of untreated and SHS-treated OPB fibers. The OPB powder sample (6–8

mg) was placed on a ceramic pan. The sample was heated from $50-550^{\circ}$ C at a heating rate of 10° C/min under nitrogen flow of 100 mL/min.

Surface Morphology Analysis

The surface morphology of untreated and SHS-treated OPB fibers was observed under a scanning electron microscopy (SEM, LEO 1455 VPSEM Electron Microscopy Ltd., Cambridge, England). For SEM analysis, oven-dried samples were mounted in the stub and gold-coated for 180s prior to the SEM observation. The SEM micrographs were obtained with an acceleration voltage of 5 kV.

RESULTS AND DISCUSSION

Chemical Composition of OPB fibers after SHS Treatment Based on Table 2, chemical composition analysis showed that the untreated OPMF contained lignin, hemicellulose and cellulose at 24, 35 and 40 wt%, respectively. Lignin composition was higher for all of the OPB fibers after the SHS treatment, while cellulose and hemicellulose composition was reduced. It was reported that SHS treatment is an effective method for hemicellulose removal from lignocellulosic samples (Nordin et al., 2013). Meanwhile, it was demonstrated earlier that SHS treatment affected cellulose content due to thermal degradation of cellulose (Warid et al., 2016). Lignin composition was higher after SHS treatment as the result of cellulose and hemicellulose weight reduction. The

Table 2
Lignocellulose composition of OPB fibers after SHS treatment

| | Fiber | Lignin Content (%) | Hemicellulose Content (%) | Cellulose Content (%) |
|-------|----------------|--------------------|---------------------------|-----------------------|
| ODME | Untreated | 24.41 ± 3.01 | 35.20 ± 1.36 | 40.39 ± 1.74 |
| OPMF | 265°C / 5 mins | 50.40 ± 1.21 | 9.88 ± 1.01 | 39.71 ± 0.20 |
| OPEED | Untreated | 14.53 ± 2.23 | 36.58 ± 2.27 | 48.89 ± 4.50 |
| OPEFB | 280°C / 5 mins | 40.49 ± 3.65 | 13.17 ± 2.03 | 46.34 ± 5.67 |
| ODE | Untreated | 14.84 ± 1.21 | 34.14 ± 5.71 | 51.02 ± 4.72 |
| OPF | 300°C / 9 mins | 40.49 ± 0.13 | 9.62 ± 3.29 | 49.89 ± 3.42 |

complexity of lignin structure makes it difficult to be degraded, apart from having wide range of thermal degradation temperature which is from 190 to 900°C. This explains the increased in lignin composition after SHS treatment.

Mechanical Properties of OPB Biocomposites

Tensile Properties of Biocomposites. The effectiveness of SHS-treated OPB fibers as reinforcement material in biocomposites can be determined by comparing mechanical properties of SHS-treated OPB/PP biocomposites and untreated OPB/PP biocomposites. Figure 1 shows the tensile strength (TS) and tensile modulus (TM) of both untreated and SHS-treated OPB/PP biocomposites, and PP was used as the control. The TS and TM of PP composites were reported to be about 40 Mpa and 7532 MPa,

respectively. In general, the addition of OPB fibers (treated and untreated) into the PP composite reduced the TS. TS is the measurement of the force required to pull material to the point where it breaks. In other words, TS of a material is the maximum amount of stress that it can take before failure, for example in this case, breaking into two. TS of OPB/PP biocomposites reduced

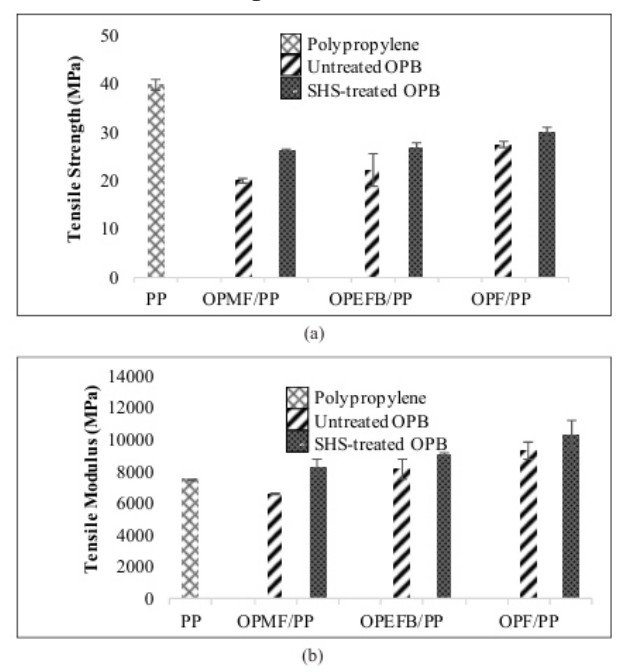


Figure 1. (a) Tensile strength (MPa) and (b) Tensile modulus (MPa) of OPB biocomposites

as low as 50% compared to TS of PP composite due to poor interfacial adhesion between hydrophobic PP and hydrophilic OPB fibers. This is due to the disruption in structural integrity of PP by the introduction of the fibers (Norrrahim, 2018).

It is interesting to note that TM of the OPB/PP biocomposites were higher compared to that of neat PP, for both untreated and SHS-treated OPB. TM can be explained as the ratio of the pressure on the material (stress) to the strain of the material. In other words, it measures the stiffness of the material. Since fibers are usually stiffer compared to polymer, the addition of OPB fibers into the PP composite caused an increment in TM. The effect of SHS treatment can be seen in all OPB fiber samples whereby the TS and TM values for all samples were increased when SHS-treated OPB was used as compared to untreated OPB. This can be explained by the improvement in hydrophobicity of the SHStreated OPB fibers as a result of hemicellulose removal, which contributed to improved compatibility and interfacial adhesion between SHS-treated OPB fibers and PP. Apart from that, SHS treatment improved the adhesive characteristics of OPB fibers by removing impurities covering the surface of the fiber, resulted in fibers with relatively clean and rough surface which are favourable for fibers-polymer interaction (Nordin et al., 2017). All of these reasons contributed to the increase in both TS and TM of SHS-treated OPB/PP biocomposites compared to untreated OPB/PP biocomposites. OPF/PP biocomposites showed the highest TS and TM at 29.8 MPa and 10303 MPa, respectively. This was followed by OPEFB/PP

biocomposites with TS and TM of 26.8 MPa and 9050 MPa, respectively, and finally OPMF/PP biocomposites (TS of 26 MPa and TM of 8273 Mpa). The difference in cellulose composition after SHS treatment (Table 1)

is expected to be the main reason which contributed to this observation. SHS-treated OPF which contained the highest cellulose showed the best mechanical properties compared to OPEFB and OPF. It is well-known that cellulose contains crystalline portion which provides strength to the biocomposite, and hence the results obtained. Based on this, it can be suggested that OPF is a superior OPB to be used as filler to improve the mechanical properties of PP biocomposite, as compared to OPMF and OPEFB.

Flexural Properties of Biocomposites. Figure 2 shows the flexural strength (FS) and flexural modulus (FM) of both untreated and SHS-treated OPB/PP biocomposites. Neat PP which was used as benchmarked sample had FS and FM of 47 MPa and 1524 Mpa, respectively. Overall, all OPB/PP biocomposite samples had lower FS, but higher FM compared to neat PP. In all cases, SHS-treated OPB/PP had higher FS and FM values compared to untreated OPB/PP. This can be explained by better compatibility of SHStreated OPB with PP as compared to untreated OPB, due to the removal of which caused partial removal of hydrophilic component. This ultimately improved interfacial adhesion between SHS-treated OPB fibers and PP matrix which in turn produced

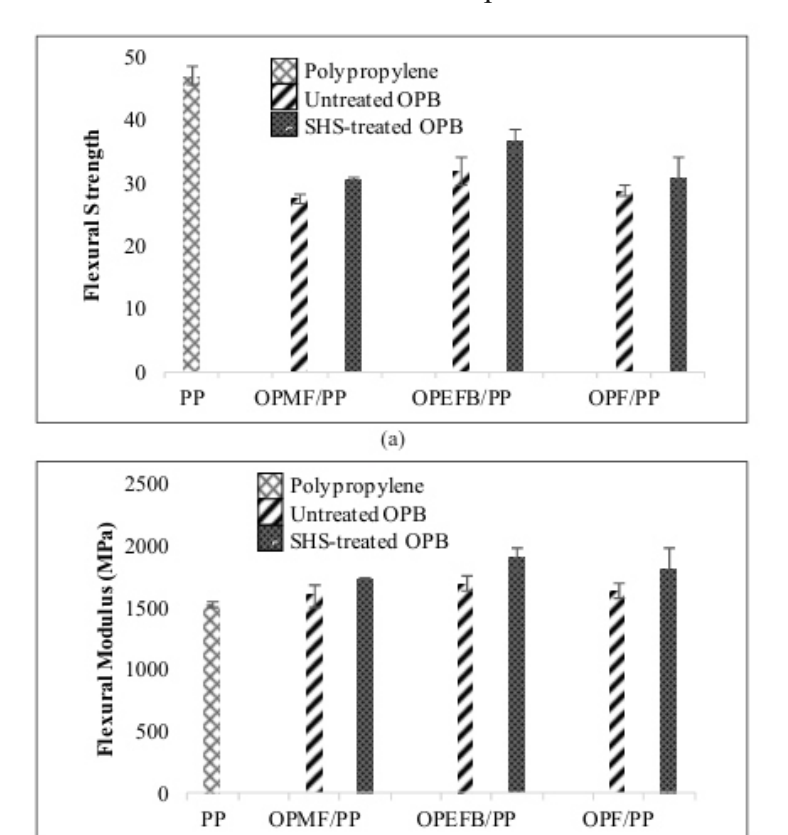


Figure 2. (a) Flexural strength (MPa) and (b) Flexural modulus (MPa) of OPB biocomposites.

biocomposite with better bending and crack propagation resistance (Nordin et al., 2017). On the other hand, segmental movement of the polymer chains can be hindered when natural fibers are introduced

(b)

into the polymer matrix and this caused the biocomposites to become stiffer and eventually improved the FM as compared to neat PP. Thermal Stability of Biocomposites. The thermal stability of biocomposites was evaluated via thermogravimetric (TG) analysis. TG thermograms of PP and OPB/PP biocomposites are illustrated in Figure 3. The information of degradation temperature at 10 and 50% weight loss, temperature at maximum rate degradation, percentage of weight loss and percentage of residual left at 500°C can be interpreted from the thermograms. Detailed interpretations are tabulated in Tables 3.

Degradation temperature at T10% was used to determine the thermal stability of the biocomposites. It is seen from Figure 3 and Table 3, thermal stability of the SHStreated OPB/PP biocomposites were higher in comparison with the untreated OPB/PP biocomposites. The removal of hemicellulose, which possesses the lowest degradation temperature among other lignocellulosic components have increased the thermal stability of the SHS-treated fibers and eventually increased the thermal stability of the biocomposites (Nordin et al., 2017).

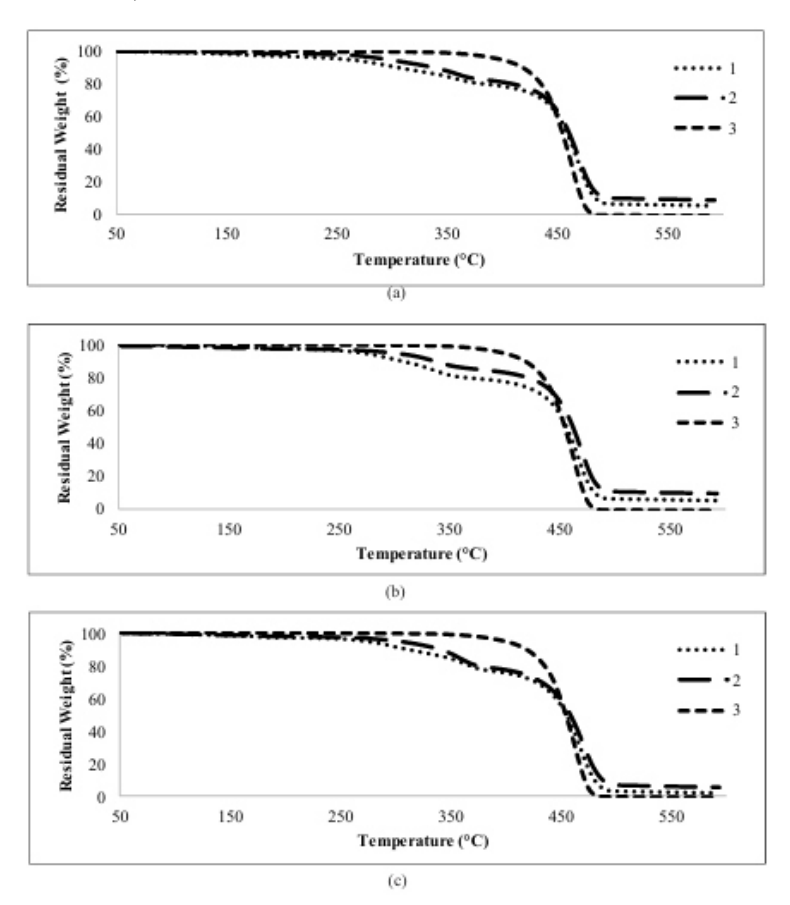


Figure 3. TG thermogram of (a) OPMF biocomposite, (b) OPEFB biocomposite and (c) OPF biocomposite Untreated OPB is labelled as (1), SHS-treated OPB (2) and Polypropylene (3)

Table 3

Thermal degradation temperature at 10% fiber degradation as shown by TG thermogram

| Bioco | mposite | Degradation temperature (°C), Tro | Residual weight at 500°C (% |
|-------|-----------|-----------------------------------|-----------------------------|
| OBME | Untreated | 305 | 6.1 |
| OPMF | Treated | 337 | 9.9 |
| OBEED | Untreated | 307 | 6.3 |
| OPEFB | Treated | 339 | 10.3 |
| ODE | Untreated | 302 | 3.5 |
| OPF | Treated | 339 | 6.6 |

Residual weight at 500°C can be related to the char formation of the biocomposites which is directly correlated to the potency of flame retardation. SHS-treated-OPEFB/PP biocomposite has the highest residue content, which is 10.3%, followed by SHS-treated OPMF/PP biocompsite (9.9%) and SHS-treated OPMF/PP biocompsite (6.6%).

Surface Morphology of Biocomposites. The tensile fractured surface of untreated and SHS-treated OPB/PP biocomposites were analyzed using a scanning electron microscope in order to determine the adhesion behaviour between untreated and SHS-treated OPB f ibers with PP matrix. Figure 4 shows the scanning electron micrographs of tensile fractured surfaces of untreated and SHS-treated OPB/PP biocomposites. These tensile fractured surface micrographs can provide useful information regarding the failure mechanism under tensile load for the corresponding biocomposites.

The SEM micrographs of untreated OPB/PP biocomposites clearly show the gaps on the OPB/PP caused by the de-bonding of fibers from polymer matrix during the tensile test. Apart from that, cavities are also observed which can be explained by the fiber pull-out during tensile test. This may be attributed by the poor interfacial adhesion due to incompatibility between hydrophilic OPB fibers and hydrophobic PP matrix. The incompatibility can also be represented by the heterogenous structure where OPB fibers and PP matrix can be easily distinguished in the micrographs. Poor interfacial adhesion eventually resulted in the premature failure as a result of poor stress transfer across the fiber-matrix interface (Nordin et al., 2013b; Warid et al., 2016; Yasim-Anuar et al., 2019). Hence, this explains the decrease in tensile and flexural strength of the biocomposites.

On the other hand, SHS-treated OPB/PP biocomposites exhibited better compatibility as shown by the scarcuty or absence of gaps and cavities on the SHS-treated OPB/PP interface region. The removal of hemicellulose during SHS treatment of OPB fibers had improved the hydrophobicity of the fibers which then enhanced the interaction with the hydrophobic PP matrix. SHS treatment also caused the removal of silica and waxy layers from the surface of OPB fibers (Nordin et al., 2013) which provided rougher surface of f ibers which can be exploited by the PP matrix for a better mechanical interlocking during biocomposite fabrication and subsequently reduced the number of fiber pull-out during tensile test.

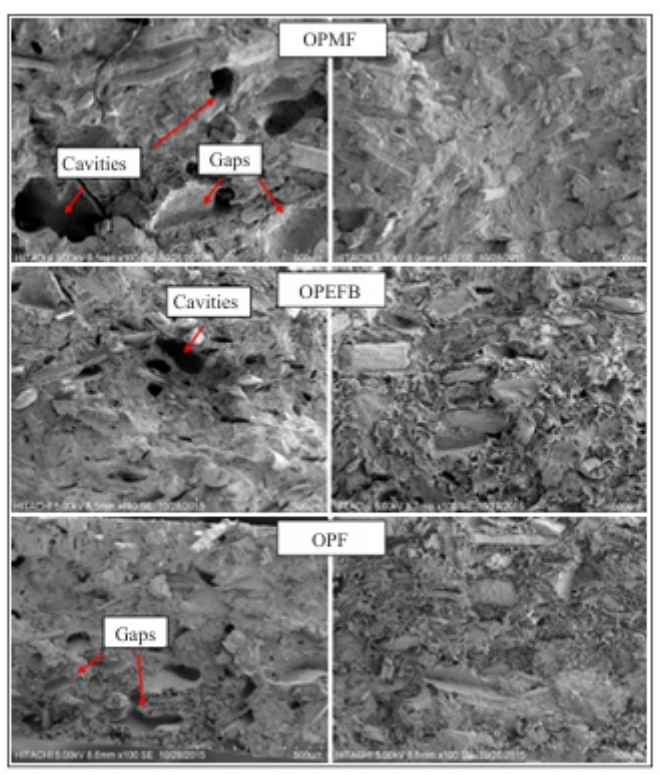


Figure 4. SEM micrographs of tensile fractured surface of untreated (L) and SHS-treated (R) OPB/PP biocomposites

CONCLUSIONS

The properties of the OPB/biocomposites were greatly affected by the types of oil palm biomass used, as well as the treatment of the fiber by SHS. Overall, OPF exhibited better performance in term of mechanical properties. This is contributed by the higher cellulose content in the OPF, the highly crystalline component in lignocellulose which could improve the mechanical properties of the biocomposites prepared using OPF as the filler. On the other hand, SHS treatment greatly affected both the mechanical and thermal properties of the SHS-treated OPB biocomposites as compared to the untreated OPB biocomposites. The removal of hemicellulose during SHS treatment improved the compatibility of the OPB with PP, contributing to better mechanical properties. The removal of hemicellulose also improved the thermal stability of the biocomposites as hemicellulose is the least stable component in lignocellulose.

ACKNOWLEDGEMENT

The authors would like to acknowledge the Ministry of Higher Education, Malaysia, and Universiti Putra Malaysia (UPM), for the financial support. The authors also would like to thank Forest Research Institute Malaysia (FRIM) for the technical support throughout the experiments and to Taman Pertanian Universiti (TPU) UPM and Seri Ulu Langat Palm Oil Mill, Selangor for the raw material supply.

REFERENCES

Abdullah, S. S. S., Shirai, Y., Bahrin, E. K., & Hassan, M. A. (2015). Fresh oil palm frond juice as a renewable, non-food, non-cellulosic and complete medium for direct bioethanol production. Industrial Crops and Products 63, 357-361. doi:10.1016/j.indcrop.2014.10.006

Acha, B. A., Reboredo, M. M., & Marcovich, N. E. (2007). Creep and dynamic mechanical behavior of PP–jute composites: Effect of the interfacial adhesion. Composites Part A: Applied Science and Manufacturing, 38(6), 1507–1516. doi:10.1016/j.compositesa.2007.01.003

Akil, H., Omar, M. F., Mazuki, A. A. M., Safiee, S. Z. A. M., Ishak, Z. M., & Bakar, A. A. (2011). Kenaffiber reinforced composites: A review. Materials & Design, 32(8-9), 4107-4121. doi:10.1016/j. matdes.2011.04.008

Bogoeva-Gaceva, G., Avella, M., Malinconico, M., Buzarovska, A., Grozdanov, A., Gentile, G., & Errico, M. E. (2007). Natural fiber eco-composites. Polymer Composites, 28(1), 98 – 107. doi:10.1002/pc.20270

Karuppuchamy, S., Andou, Y., Nishida, H., Nordin, N. I. A. A., Ariffin, H., Hassan, M. A., & Shirai, Y. (2015). Superheated steam treated oil palm frond fibers and their application in plastic composites. Advanced Science, Engineering and Medicine, 7(2), 120–125. doi:10.1166/asem.2015.1659

Nordin, N. I. A. A., Ariffin, H., Hassan, M. A., Shirai, Y., Ando, Y., Ibrahim, N. A., & Yunus, W. M. Z. W. (2017).

Superheated steam treatment of oil palm mesocarp fiber improved the properties of fiber-polypropylene biocomposite. BioResources, 12(1), 68-81. doi:10.15376/biores.12.1.68-81

Nordin, N. I. A. A., Ariffin, H., Andou, Y., Hassan, M. A., Shirai, Y., Nishida, H., & Ibrahim, N. A. (2013). Modification of oil palm mesocarp fiber characteristics using superheated steam treatment. Molecules, 18(8), 9132–9146. doi:10.3390/molecules18089132

Norrrahim, M. N. F. (2018) Superheated steam pretreatment of oil palm biomass for improving nanofibrillation

of cellulose and performance of polypropylene / cellulose nanofiber composites. (Doctoral thesis) Universiti Putra Malaysia, Malaysia.

Raju, C., Ratnam, C. T., Ibrahim, N. A., Rahman, M. Z. A., & Yunus, W. M. Z. W. (2008). Enhancement of PVC/ENR blend properties by poly (methyl acrylate) grafted oil palm empty fruit bunch fiber. Journal of Applied Polymer Science, 110(1), 368–375. doi:10.1002/app.28662

Spoljaric, S., Genovese, A., & Shanks, R. A. (2009). Polypropylene–microcrystalline cellulose composites with enhanced compatibility and properties. Composites Part A: Applied Science and Manufacturing, 40(6-7), 791–799. doi:10.1016/j.compositesa.2009.03.011

Then, Y. Y., Ibrahim, N. A., Zainuddin, N., Ariffin, H., & Yunus, W. M. Z. W (2013). Oil palm mesocarp fiber as new lignocellulosic material for fabrication of polymer/fiber biocomposites. International Journal of Polymer Science, 2013, 1–7. doi:10.1155/2013/797452

Warid, M. N. M., Ariffin, H., Hassan, M. A., & Shirai, Y. (2016). Optimization of superheated steam treatment to improve surface modification of oil palm biomass fiber. BioResources, 11(3), 5780-5796. doi:10.15376/biores.11.3.5780-5796

Yasim-Anuar, T. A. T., Ariffin, H., Norrrahim, M. N. F., Hassan, M. A., Andou, Y., Tsukegi, T., & Nishida, H. (2020). Well-dispersed cellulose nanofiber in low density polyethylene nanocomposite by liquid-assisted extrusion. Polymers, 12(4), 1-17. doi:10.3390/polym12040927

Yasim-Anuar, T. A. T., Ariffin, H., Norrrahim, M. N. F., Hassan, M. A., Tsukegi, T., & Nishida, H. (2019). Sustainable one-pot process for the production of cellulose nanofiber and polyethylene/cellulose nanofiber composites. Journal of Cleaner Production, 207, 590-599. doi:10.1016/j.jclepro.2018.09.266

Parameters Optimization in Compression Molding of Ultra high Molecular Weight Polyethylene/Cellulose Nanofiber Bio nanocomposites by using Response Surface Methodology

Nur Sharmila Sharip1, Hidayah Ariffin1,2*, Yoshito Andou3, Ezyana Kamal Bahrin2, Mohammad Jawaid4, Paridah Md Tahir5 and Nor Azowa Ibrahim6

1 Laboratory of Biopolymer and Derivatives, Institute of Tropical Forestry and Forest Products (INTROP), Universiti Putra Malaysia, 43400 UPM Serdang, Selangor, Malaysia

2Department of Bioprocess Technology, Faculty of Biotechnology and Biomolecular Sciences, Universiti Putra Malaysia, 43400 UPM Serdang, Selangor, Malaysia 3Department of Biological Functions and Engineering, Graduate School of Life Science and Systems Engineering, Kyushu Institute of Technology, 2-4 Hibikino, Wakamatsu-ku, Kitakyushu, Fukuoka 808-0196, Japan

4Laboratory of Biocomposite Technology, Institute of Tropical Forestry and Forest Products (INTROP), Universiti Putra Malaysia, 43400 UPM Serdang, Selangor, Malaysia

5Laboratory of Sustainable Bioresource Management, Institute of Tropical Forestry and Forest Products (INTROP), Universiti Putra Malaysia, 43400 UPM Serdang, Selangor, Malaysia

6Department of Chemistry, Faculty of Sciences, Universiti Putra Malaysia, 43400 UPM Serdang, Selangor, Malaysia

ABSTRACT

Conventional UHMWPE molding involves long pressure holding duration, nevertheless in the presence of filler such as cellulose nanofiber (CNF), this may contribute to filler degradation. This study optimized the compression molding parameters of UHMWPE/CNF bio-nanocomposite by using response surface methodology (RSM) in consideration of temperature, pressure and duration as variables. An optimal processing condition of 180°C, 15 MPa, and 20 minutes contributed to more than 80% desirability with tensile strength, yield strength, elongation at break, and Young's modulus values of 22.83 MPa, 23.14 MPa, 487.31%, and 0.391 GPa, accordingly. Mechanical properties of UHMWPE/CNF bio-nanocomposites molded at optimized processing conditions were comparably similar to those prepared at conventional processing condition, and with the advantage of having shorter processing time. The results presented herewith provides insight towards a more practical approach for UHMWPE/CNF bio-nanocomposites consolidation process.

Keywords: Bio-nanocomposite, cellulose nanofiber, compression molding, optimization, response surface methodology, ultra-high molecular weight polyethylene

INTRODUCTION

Possessing various excellent properties, ultra-high molecular weight polyethylene (UHMWPE) has been used for various application of aerospace, industrial machineries, microelectronic and medical fields (Li et al., 2017; Raghuvanshi et al., 2012), where it is consolidated into many different products

including pipes, panels, gears, body armors, unlubricated bearings and artificial joint component (Khalil et al., 2016; Wang et al., 2018). This engineered thermoplastic is made of a repeating unit of ethylene with molecular weight ranged between 3.5 to 7.5 million g/mol (Kurtz, 2016a). The extremely long and linear structure of UHMWPE enables it to greatly withstand impact and abrasion beside having a very low friction (Chukov et al., 2014; Paxton et al., 2019). Not only that, a lot of studies have been conducted on manufacturing UHMWPE nanocomposites for enhanced properties befitting its applications, including UHMWPE/nanocellulose as artificial joint component (Wang et al., 2016).

While various approaches can be adopted in manufacturing and processing the UHMWPE and/or its composites, the consolidation process is restricted to compression molding and ram extrusion. This is stemmed from very low melt flow index of UHMWPE (0.006 g/min) causing other methods such as injection molding and screw extrusion to be not practical (Kurtz, 2016b; Panin et al., 2017). In comparison to other consolidation method, compression molding is considered more practical and well adapted, especially for molding UHMWPE polymer. Differing from other polymers including conventional polyethylene such as low-density polyethylene or high-density polyethylene, UHMWPE comprises extremely long chains leading to very high melt viscosity and slow diffusion during consolidation (Fu et al., 2010; Gao & Fu, 2019). Hence, UHMWPE molding requires a long pressure holding duration, in order to give adequate time for UHMWPE resin to diffuse with each other and create satisfactory entanglements thus good mechanical properties (Kurtz et al., 1999; Parasnis & Ramani, 1998). Besides, Kurtz (2016b) further described that long duration of hot pressing was necessary due to the relatively low thermal conductivity of UHMWPE.

Nevertheless, long duration molding could be a disadvantage, which may expose polymer to degradation (Campo, 2008), especially in consolidation of UHMWPE containing cellulose nanofiber (CNF) fillers. Appropriate compression molding parameters are essentially needed for polymer diffusion and filler impregnation into the matrix (Xie et al., 2019) while avoiding polymer degradation. Meanwhile, in order to improve its productivity, the shorter duration is imperative for more effective processing. The effect, conjugated with interaction between the varied parameters, wields an impact towards the quality and mechanical properties of UHMWPE/CNF bio-nanocomposites. Therefore, this study optimized the temperature pressure and duration of compression molding for desirably good mechanical properties. The individual and interaction effects of each variables on UHMWPE/CNF bio-nanocomposites mechanical properties were also investigated.

MATERIALS AND METHODS

Materials

Fine UHMWPE powder (Sigma-Aldrich, USA) with average molecular weight of 3 x 106 – 6 x 106

g/mol was used in this experiment. Maleic anhydride-grafted-polyethylene (MAPE) in pellet form was from the same manufacturer by which it contains approximately 0.5 wt.% maleic anhydride. The melting point and density of UHMWPE and MAPE are 138°C, 0.94 g/mL and 107°C, 0.92 g/mL, respectively. The CNF in slurry form was purchased from ZoepNano Sdn. Bhd., Malaysia with concentration of 2 wt.% solid content and average diameter of 50 nm.

Bio-nanocomposite Fabrication and Molding

UHMWPE/ 3 wt.% CNF/ 3 wt.% MAPE bio-nanocomposite was prepared by using triple screw kneading extruder (Imoto Machinery Co., Ltd., Japan) at temperature 150°C, 60 rpm and 45 minutes melt blending condition. Fabricated bio-nanocomposite was then subjected to compression molding at varied parameters of temperature, pressure and duration.

Mechanical Properties of Bio-nanocomposites

Tensile specimen was prepared from compressed bio-nanocomposite film according to ASTM D638. The test was conducted on compact tensile and compression tester IMC18E0 (Imoto Machinery Co., Ltd., Japan) at 50 mm/min crosshead speed) (ASTM, 2003). The mechanical properties of bio-nanocomposites after the validation experiment was analyzed using one-way ANOVA and Duncan's multiple range test for statistical analysis.

Experiment Design and Optimization

Compression molding parameters were optimized by using face-centered central composite design (CCD) of response surface methodology (RSM). Varied parameters or variables are molding temperature (X1), pressure (X2), and duration (X3) with a range of 150 to 200°C, 10 to 20 MPa, and 20 to 100 minutes, accordingly. The effect of variables on mechanical properties was investigated through determination of tensile strength (Y1), yield strength (Y2), elongation at break (Y3), and Young's modulus (Y4) as responses. The coded values of three operating variables were set at three levels: -1 (minimum), 0 (central), and +1 (maximum) as shown in Table 1. A total of 20 experiments (2k + 2k + 6) inclusive of 8 factorial points, 6 axial points and 6 center points were conducted where the alpha was set to one.

Data were analyzed by using Design Expert statistical software (Version 7.0, StatEase Inc. Minneapolis, MN, USA) where the significance of each variable and regression coefficients were evaluated by considering more than 95% confidence level (P<0.05) of variance analysis (ANOVA). The effect of variable on the responses was expressed in dimensional (3D) and contour plot response surface in order to locate the optimal level. A second order polynomial equation was used to explain the system behavior as shown in Equation 1 where Y1, Y2, Y3, and Y4 are the responses and X1, X2, and X3 are the variables influencing Y as response. The β 0 is the constant coefficient; β 1, β 2, β 3 are linear coefficients; β 1, β 23 are interaction coefficients; and β 11, β 22, β 33 are quadratic coefficients.

 $Y = \beta 0 + \beta 1 X 1 + \beta 2 X 2 + \beta 3 X 3 + \beta 12 X 1 X 2 + \beta 13 X 1 X 3 + \beta 23 X 2 X 3 + \beta 11 X 12 + \beta 22 X 22 + \beta 33 X 32$ (Equation 1)

Table 1 Central composite design matrix of coded and actual level of variables

| D | Temperatu | re (°C), X ₁ | Pressure | $(MPa), X_2$ | Duration | (min), X ₃ |
|-----|-----------|-------------------------|----------|--------------|----------|-----------------------|
| Run | Coded | Actual | Coded | Actual | Coded | Actual |
| 1 | 0 | 175 | 0 | 15 | 0 | 60 |
| 2 | +1 | 200 | -1 | 10 | +1 | 100 |
| 3 | 0 | 175 | 0 | 15 | 0 | 60 |
| 4 | 0 | 175 | +1 | 20 | 0 | 60 |
| 5 | 0 | 175 | 0 | 15 | -1 | 20 |
| 6 | 0 | 175 | 0 | 15 | 0 | 60 |
| 7 | -1 | 150 | -1 | 10 | +1 | 100 |
| 8 | 0 | 175 | 0 | 15 | 0 | 60 |
| 9 | -1 | 150 | +1 | 20 | +1 | 100 |
| 10 | +1 | 200 | +1 | 20 | +1 | 100 |
| 11 | +1 | 200 | +1 | 20 | -1 | 20 |
| 12 | -1 | 150 | 0 | 15 | 0 | 60 |
| 13 | +1 | 200 | -1 | 10 | -1 | 20 |
| 14 | 0 | 175 | 0 | 15 | +1 | 100 |
| 15 | 0 | 175 | 0 | 15 | 0 | 60 |
| 16 | +1 | 200 | 0 | 15 | 0 | 60 |
| 17 | 0 | 175 | -1 | 10 | 0 | 60 |
| 18 | -1 | 150 | -1 | 10 | -1 | 20 |
| 19 | 0 | 175 | 0 | 15 | 0 | 60 |
| 20 | -1 | 150 | +1 | 20 | -1 | 20 |

Validation Experiment and Verification

The validity and adequacy of the regression models were proven by comparing the experimental data obtained and the fitted value predicted by the models.

RESULTS AND DISCUSSION

Preliminary Experiment and Range Selection

Selection of range was in accordance to the preliminary experiment of one-variable-at time (OVAT) for molding duration, while temperature and pressure were selected based on literature. Temperature was ranged between 150°C to 200°C in consideration to melting temperature of UHMWPE which is approximately 140°C (Oral & Muratoglu, 2016) and the degradation temperature of CNF which is around 220°C (Yasim-Anuar et al., 2018).

This is because cellulose degradation at high temperature could reduce the stiffness and strength of cellulose composite (Forsgren et al., 2020; Sapieha et al., 1989). Meanwhile, cellulose degradation was negligible at temperature below 200°C (Le Baillif & Oksman, 2009; Gan et al., 2020). Pressure range was set at 10 to 20 MPa as according to Wang & Ge (2007) and the range of duration was selected from 20

to 100 minutes based on the OVAT experiment conducted as shown in Figure 1. High tensile strength and elongation at break of UHMWPE/CNF bio-nanocomposites indicating less voids between UHMWPE granules and sufficient molding time were obtained after 20 minutes molding. Gradual reduction of elongation at break observed through further prolonged duration (60 to 100 minutes) proved appropriate selection of 60 minutes as a center point in between 20 to 100 minutes.

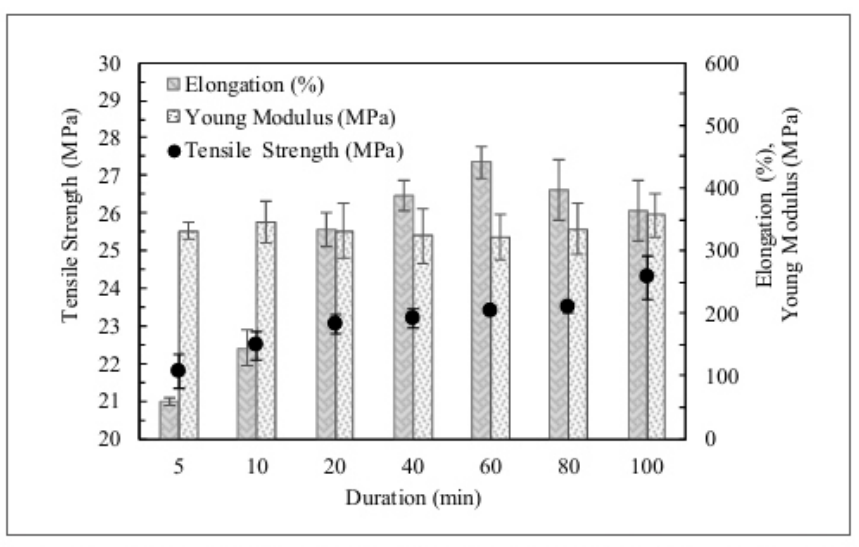


Figure 1. Mechanical properties of UHMWPE/CNF bio-nanocomposites as affected by duration at 175 °C and 15 MPa compression molding

Model Analysis

Table 2 shows the experimental and predicted values of the responses; tensile strength (Y1), yield strength (Y2), elongation at break (Y3) and Young's modulus (Y4). Natural log transformation was applied on elongation response as the best transformation suggested by the software. This was in consideration to the high maximum to minimum ratio of Y3, values that were more than three (3.204). The values obtained from Table 2 were subjected to analysis of variance (ANOVA) in order to select the model for each response, depending on the resulted significant model probability (P<0.05), insignificant lack-of-fit probability (P>0.05) and more than 80% coefficient of determination (R2) (Bagheri et al., 2019; Warid et al., 2016). Full quadratic model was adopted as the best-fitted model where the results of ANOVA is tabulated in Table 3.

All models were found significant at the 5% confidence level where the p-values were all less than 0.05. The insignificant lack-of fit value (P>0.05) of all response models (0.9161,

Table 2
Experimental and predicted values of responses

| Run | | strength a), Y ₁ | Yield si (MP | | Elongat Y | | | modulus a), Y ₄ |
|-----|------|--------------------------------|-----------------|--------|--------------|--------|-------|-------------------------------|
| | *Exp | **Pred | *Exp | **Pred | *Exp | **Pred | *Exp | **Pred |
| 1 | 25.4 | 24.8 | 22.6 | 22.7 | 480.3 | 457.6 | 0.346 | 0.343 |
| 2 | 22.8 | 22.9 | 23.1 | 23.1 | 243.8 | 238.7 | 0.361 | 0.356 |
| 3 | 25.1 | 24.8 | 22.7 | 22.7 | 473.1 | 457.6 | 0.341 | 0.343 |
| 4 | 24.3 | 24.3 | 22.5 | 22.7 | 393.9 | 397.4 | 0.334 | 0.337 |
| 5 | 25.0 | 24.8 | 22.7 | 22.7 | 425.3 | 436.7 | 0.347 | 0.344 |
| 6 | 23.5 | 24.8 | 22.9 | 22.7 | 455.7 | 457.6 | 0.341 | 0.343 |
| 7 | 25.9 | 25.9 | 21.4 | 21.3 | 299.0 | 294.6 | 0.325 | 0.333 |
| 8 | 25.0 | 24.8 | 22.7 | 22.7 | 496.8 | 457.6 | 0.333 | 0.343 |
| 9 | 27.1 | 27.4 | 21.3 | 21.3 | 371.9 | 366.8 | 0.322 | 0.320 |
| 10 | 22.8 | 22.5 | 23.1 | 23.1 | 155.1 | 155.8 | 0.378 | 0.378 |
| 11 | 23.6 | 23.7 | 23.3 | 23.2 | 216.2 | 215.5 | 0.366 | 0.359 |
| 12 | 27.3 | 26.9 | 21.4 | 21.6 | 385.8 | 404.7 | 0.353 | 0.341 |
| 13 | 23.7 | 23.5 | 23.5 | 23.5 | 274.4 | 273.3 | 0.359 | 0.362 |
| 14 | 24.8 | 24.9 | 22.2 | 22.4 | 380.5 | 398.0 | 0.339 | 0.338 |
| 15 | 24.3 | 24.8 | 23.3 | 22.7 | 468.3 | 457.6 | 0.349 | 0.343 |
| 16 | 23.7 | 24.0 | 23.2 | 23.3 | 265.9 | 272.2 | 0.361 | 0.369 |
| 17 | 23.5 | 23.4 | 22.9 | 22.9 | 376.7 | 401.0 | 0.351 | 0.344 |
| 18 | 24.1 | 24.4 | 22.0 | 21.9 | 262.4 | 256.5 | 0.364 | 0.364 |
| 19 | 25.0 | 24.8 | 22.7 | 22.7 | 440.0 | 457.6 | 0.340 | 0.343 |
| 20 | 26.6 | 26.5 | 21.6 | 21.6 | 384.6 | 385.9 | 0.321 | 0.327 |

^{*}Exp: Experimental; **Pred: Predicted

Table 3
Analysis of variance (ANOVA) for response surface quadratic model

| | Tensile strength (MPa), Y ₁ | Yield strength (MPa), Y ₂ | Ln Elongation (%), Ln Y ₃ | Young's Modulus (GPa), Y ₄ |
|------------------------------|---|---|---|--|
| Model - Quadratic | 0.0006* | <0.0001* | <0.0001* | 0.0026* |
| | | Linear | | |
| X ₁ – Temperature | <0.0001* | <0.0001* | <0.0001* | 0.0002* |
| X ₂ – Pressure | 0.0357* | 0.2392 | 0.7711 | 0.1475 |
| X ₃ – Duration | 0.7930 | 0.0195* | 0.0122* | 0.2387 |
| | | Interaction | | |
| $X_1 X_2$ | 0.0407* | 0.8171 | < 0.0001* | 0.0102* |
| $X_1 X_3$ | 0.0255* | 0.6101 | 0.0025* | 0.0416* |
| $X_2 X_3$ | 0.4916 | 0.4619 | 0.0196* | 0.0463* |
| | | Quadratic | | |
| X ₁ ² | 0.0604 | 0.0548 | < 0.0001* | 0.0339* |
| X_{2}^{2} | 0.0212* | 0.4529 | 0.0008* | 0.6066 |
| $X_3^{\ 2}$ | 0.8692 | 0.2564 | 0.0094* | 0.6430 |
| Lack of Fit | 0.9161** | 0.7571** | 0.3047** | 0.1337** |
| \mathbb{R}^2 | 0.9027 | 0.9463 | 0.9876 | 0.8642 |
| Standard deviation | 0.56 | 0.22 | 0.048 | 0.0078 |
| Adequate precision | 12.183 | 14.697 | 31.60 | 10.550 |

^{*}statistically significant at p < 0.05 for model;

0.7571, 0.3047, and 0.1337, accordingly) indicated that each model could successfully predict and represent the data at points that was not included in the regression. This was also supported by high determination coefficients, R2 by which the obtained values of 0.9027, 0.9463, 0.9876, and 0.8642 implied that 90%, 95%, 99% and 86% variance proportion of tensile strength, yield strength, elongation at break and Young's modulus are predictable by the model. As shown in Figure 2, predictions of all models were in a satisfactory match with the experimental value by which the proximity points were scattered along the fitted line. Additionally, the signal-to-noise ratio (adequate precision) of all response

^{**}statistically insignificant at p > 0.05 for lack of fit test

models were of greater than four, implying an adequate signal to navigate the design space including the estimation of the standard error of the predictions (Moradi et al., 2016).

Effect of the Compression Molding Variables on the Mechanical Properties of UHMWPE/CNF Bio-nanocomposites

The estimated regression coefficient explaining the variables effect on responses were expressed in equation follows, where Y1, Y2, Y3, and Y4 represent tensile strength, yield strength, elongation at break, and Young's modulus, respectively; and X1, X2, and X3 are mixing temperature, pressure and duration, respectively.

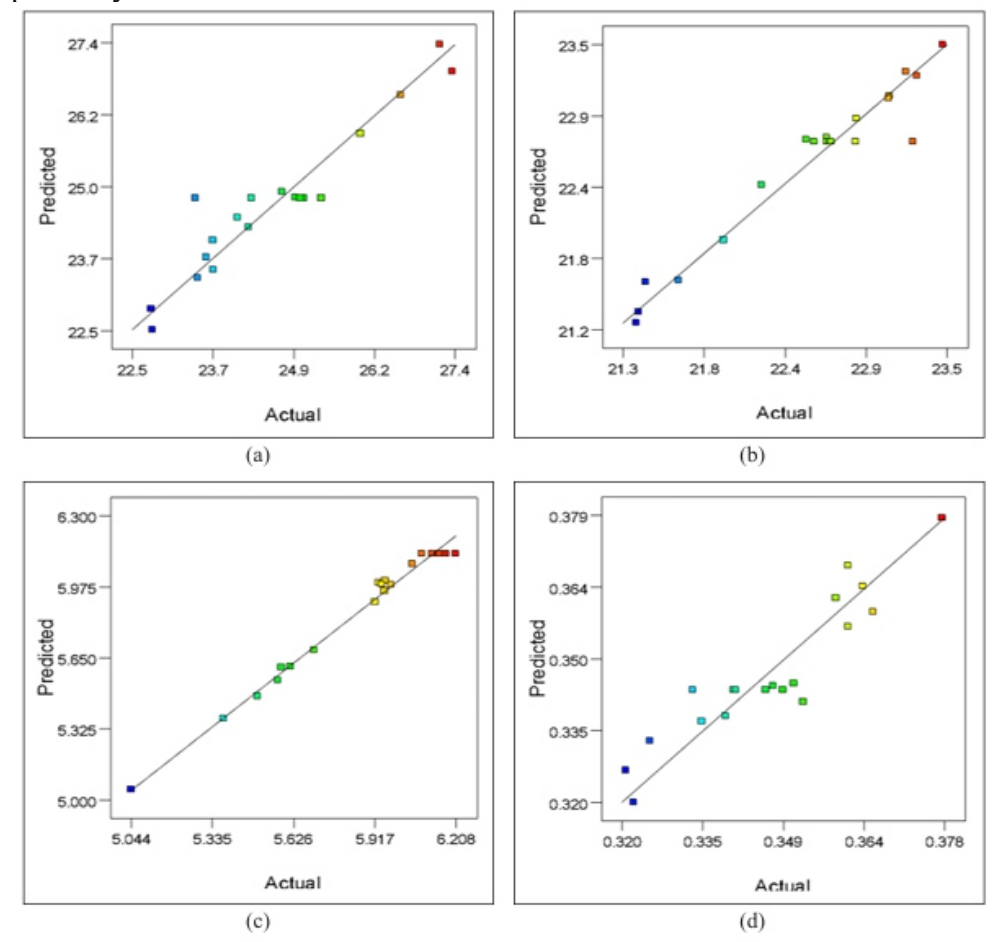


Figure 2. Experimental and predicted values for: (a) tensile strength; (b) yield strength; (c) elongation; and (d) Young's modulus of UHMWPE/CNF bio-nanocomposites

(Equation 4)

$$Y_4 = 0.34 + 0.014 X_1 - 0.0039 X_2 - 0.0031 X_3 + 0.0087 X_1 X_2 + 0.0065 X_1 X_3 + 0.0063 X_2 X_3 + 0.012 X_1^2 - 0.0025 X_2^2 - 0.0023 X_3^2$$
 (Equation 5)

A perturbation plot was used to explain the individual effect of each variables on the responses studied. For instance, the coded units shown in Figure 3 represent the range of variables from -1.0 to +1.0 (i.e. 150°C to 200°C for temperature), whereby varied temperature and pressure gave significant linear effect on tensile strength. Increased temperature caused reduction of tensile strength whereby increased pressure up to 0.5 coded unit (17.5 MPa) led to increment of the response before reduced at higher pressure beyond 17.5 MPa.

The three-dimensional and contour plot of response surface showing interaction between variables against tensile strength according to Equation 2 is shown in Figure 4. Significant interaction effect of temperature and pressure was observed in which increased temperature along with pressure remarkably reduced the tensile strength (Figure 4a). In a similar manner, increased temperature along with increased duration of molding reduced the tensile strength despite insignificant linear effect of the later variable (Figure 4b). According to Xie et al. (2019), low temperature of compression molding may lead to insufficient impregnation of fillers and adjacent polymer chains while too high a temperature can lead to degradation. Meanwhile, longer duration could beneficially affected tensile strength due to improved resin flow and better fillers impregnation. Nevertheless, too long exposure to high temperature may also lead to degradation, hence explained the findings in this study by which highest tensile strength was obtained when UHMWPE/CNF bio-nanocomposites was molded at Run 9 (150°C, 15 MPa for 60 minutes) (Table 2). On the other hand, the lowest tensile strength was recorded in Run 2 (200°C, 10 MPa for 100 minutes).

In term of yield strength, no significant interaction between all variables was observed despite significant linear effect by temperature and duration (Table 3 and Figure 5a). Increased temperature from 150°C to 200°C (-1.0 to +1.0 coded unit) notably caused increment from approximately 21 MPa to 23 MPa. Prolonged duration from 20 to 60 minutes (-1.0 to 0 coded unit) gave no effect on yield strength but reduced when molded longer up to 100 minutes (+1 coded unit), possibly due to some thermal degradation attributed to long exposure to

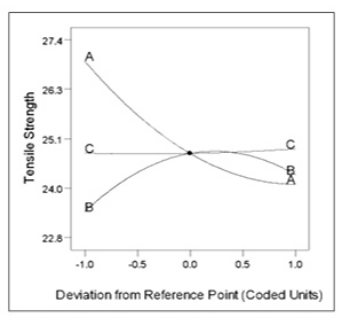


Figure 3. Perturbation plot of tensile strength in response to the changes of (A) temperature, (B) pressure, and (C) duration

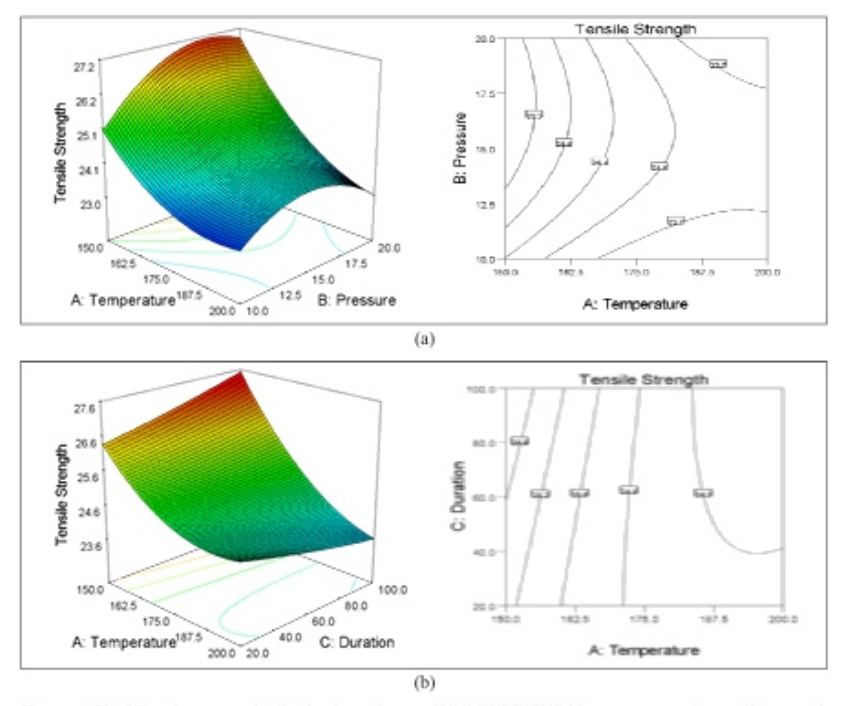


Figure 4. The 3D and contour plot for the dependence of UHMWPE/CNF bio-nanocomposite tensile strength on: (a) temperature and pressure; and (b) temperature and duration as significant variables

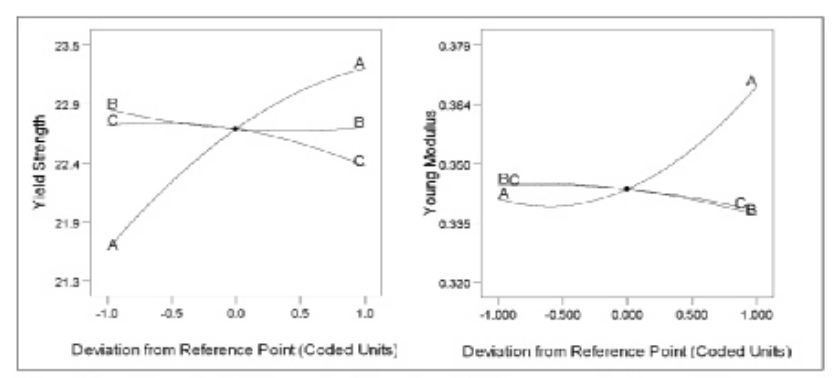
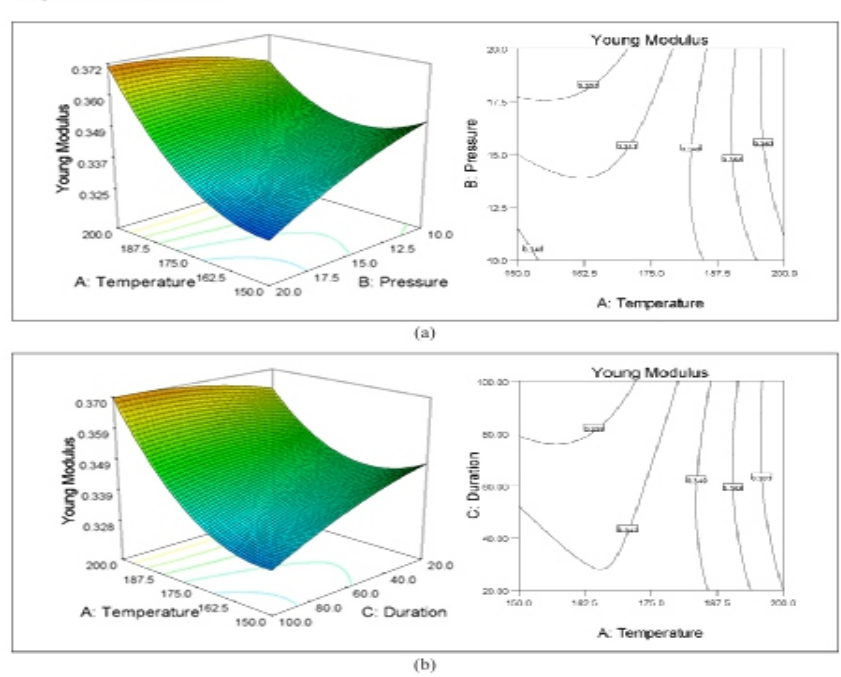


Figure 5. Perturbation plot of yield strength and Young's modulus in response to the changes of (A) temperature, (B) pressure and (C) duration



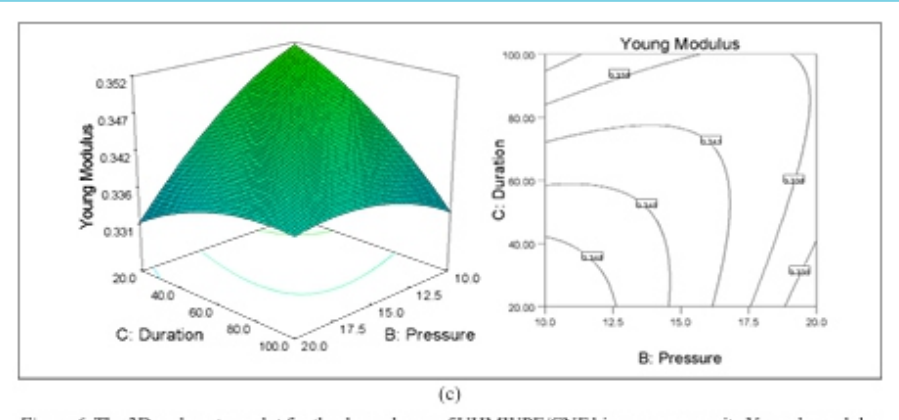


Figure 6. The 3D and contour plot for the dependence of UHMWPE/CNF bio-nanocomposite Young's modulus on: (a) temperature and pressure; (b) temperature and duration; and (c) pressure and duration as significant variables

high temperature and pressure as previously described. In contrary, Young's modulus increased with increases of temperature (Figure 5b) while other variables gave no significant linear effect. Possible UHMWPE degradation was predicted due to exposure to high temperature and pressure. As degradation of polymer leads to formation of shorter chains that enable more packed crystals arrangement (Gleadall, 2015; Riley, 2012), higher crystallinity contributes to increases in Young's modulus (Doyle, 2000; Humbert et al., 2011). The synergistic effect of temperature with pressure, and temperature with duration on Young's modulus can also be seen in Figure 6a and Figure 6b, respectively, where Young's modulus increased along with increase values of the interacted variables. Inversely, the response value decreased by increases of pressure and duration as shown in Figure 6c.

The full quadratic model adopted comprised linear, interaction and quadratic terms indicating effect of variables on the respective response. For elongation at break, all model term listed were found to be significant except for linear pressure effect (Table 3). As shown in Figure 7, increased temperature and duration positively affected this response from -1.0 (lowest range) to -0.5 (162.5°C) and 0 (60 minutes) coded values, respectively. Further increase in both variables caused decrement in elongation at break, whereas interaction between all variables were significant as illustrated in three dimensional and contour plot of elongation break in Figure 8. The responses were in higher values when molded at temperature 162.5 to 175°C, 12.5 to 17.5 MPa and 40 to 60 minutes (Figure that the optimal temperature for obtaining high elongation at break was within this range.

Response Surface Optimization of the Compression Molding Variables

Mechanical properties of UHMWPE/CNF bio-nanocomposites were notably affected by varied temperature, duration, interaction of other variables with temperature, duration, and pressure in descending order. The impact is however depended on the capability of polymer chains to undergo self diffusion that results in elimination of inter-particle voids beside avoidance of polymer degradation. An incomplete diffused UHMWPE particle/resin and CNF impregnation was expected to cause formation of voids or boundaries hence may act as cracks initiation site that afflicted the mechanical properties

including tensile strength and elongation at break. As such, optimized temperature, duration and pressure play role in

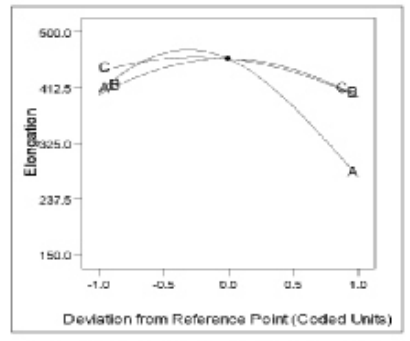


Figure 7. Perturbation plot of elongation at break in response to the changes of (A) temperature, (B) pressure and (C) duration

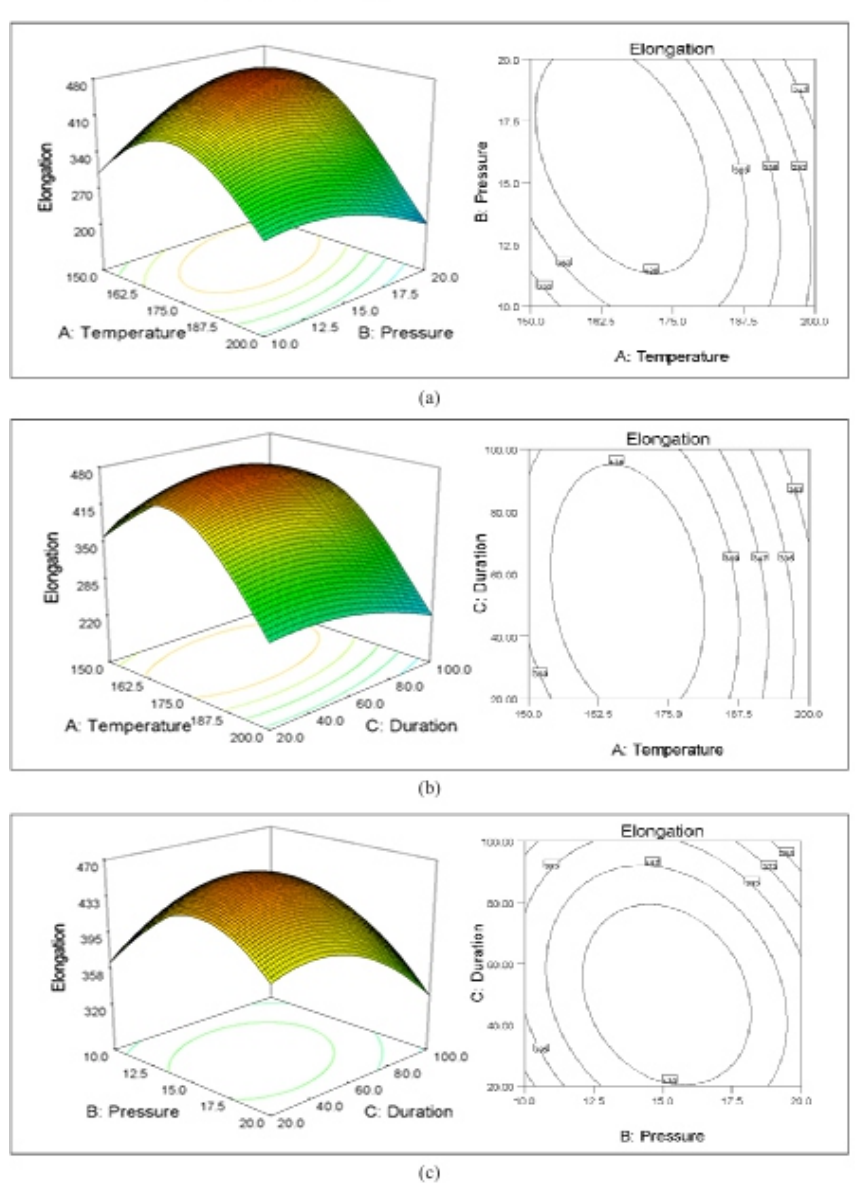


Figure 8. The 3D and contour plot for the dependence of UHMWPE/CNF bio-nanocomposite elongation at break on: (a) temperature and pressure; (b) temperature and duration; and (c) pressure and duration as significant variables

providing sufficient melt flow and time for UHMWPE polymer chains to allow complete consolidation and eliminates the boundaries through diffused adjacent chains. Additionally, adequate entanglement between adjacent chains could be established and translated into good mechanical properties.

A numerical optimization was conducted based on the design and the criteria of each variables as shown in Table 4. All mechanical properties were set to maximum except yield strength that was set in range. This was due to its small changes affected by varied temperature while other variables were insignificant. Optimum temperature, pressure and duration of compression molding were found to be at 180°C, 15 MPa and 20 minutes, respectively with desirability of 0.811. Verification experiment conducted proved the accuracy of the models where experimental value of all mechanical properties were in agreement with the predicted value by which all percent errors were less than 5% (Table 5).

Table 4 Numerical optimization criterion settings and solutions

| | | | V | ariables c | onstraint | s | | |
|---------|-------|-------------|------|------------|-----------|-------|-------|--------------|
| Name | | Goal | | Lower | limit | Upper | limit | |
| X_1 | | is in range | e | 150 | .0 | 200. | 0 | |
| X2 | | is in range | e | 10. | 0 | 20.0 |) | |
| X_3 | | minimize | | 20. | 0 | 100. | 0 | |
| | | | R | esponse c | onstraint | s | | |
| Y_1 | | maximize | | 22. | 8 | 27.3 | 3 | |
| Y2 | | is in range | e | 21. | 3 | 23.5 | 5 | |
| Y, | | maximize | : | 155 | .1 | 496. | 8 | |
| Y_{+} | | maximize | | 0.32 | 21 | 0.37 | 8 | |
| | | | C | Pptimum | Solutions | | | |
| No. | X_1 | X2 | X3 | Y_1 | Y_2 | Y3 | Y_4 | Desirability |
| 1 | 180.0 | 15.0 | 20.0 | 24.6 | 22.9 | 420.1 | 0.346 | 0.811 |
| 2 | 180.5 | 15.0 | 20.0 | 24.6 | 22.9 | 417.9 | 0.346 | 0.809 |
| 3 | 180.0 | 17.5 | 20.0 | 24.6 | 22.9 | 408.1 | 0.341 | 0.787 |
| 3 | 180.0 | 10.0 | 20.0 | 23.2 | 23.1 | 362.7 | 0.352 | 0.681 |

Table 5

Comparison between predicted and experimental values of UHMWPE/CNF bio-nanocomposites fabricated at optimal conditions

| | Predicted | Experimental | Percent error(%) |
|-------------------------------------|-----------|-------------------|------------------|
| Tensile strength (MPa), Y1 | 24.6 | 24.1 ± 1.1 | 1.92 |
| Yield Strength (MPa), Y2 | 22.9 | 23.3 ± 0.5 | 1.89 |
| Elongation (%), Y ₃ | 420.1 | 433.5 ± 26.2 | 3.22 |
| Young Modulus (GPa), Y ₄ | 0.346 | 0.361 ± 0.026 | 4.48 |

In addition, the optimized compression molding parameter obtained in this study was proven to provide comparable mechanical properties to the conventional process which required 45 minutes of molding duration. the duration of optimized condition was only 20 minutes which was less than two times shorter, hence could be favorable for industrial use (Table 6). Specifically, no significant different was observed on elongation and Young's modulus, while yield strength was only 2% higher. The tensile strength was however reduced from 28.0 MPa to 24.1 MPa.

Materials often experienced yielding, inelastic and plastic deformation before rupture. In order, the ability of materials to withstand load and undergo changes is determine through yield strength, Young's modulus and tensile strength. In light of UHMWPE utilization as load bearing materials such as joint

arthroplasty component, yield strength is considered more important than tensile strength by which materials yielding under service condition is considered a failure (Fang et al., 2006). Moreover, the mechanical properties obtained from optimized molding conditions surpassed the minimal requirement of standard specification for consolidated UHMWPE for surgical implant (ASTM F648) which are 27 MPa, 19 Mpa, and 250 % of tensile strength, yield strength and elongation, respectively (ASTM, 2014).

Table 6 Comparison between conventional and optimized compression molding

| | Conventional (Kurtz et al., 1999) | Optimized (This study) |
|------------------------|-----------------------------------|--------------------------|
| Temperature (°C) | 175 | 180 |
| Pressure (MPa) | 15 | 15 |
| Duration (min) | 45 | 20 |
| Tensile strength (MPa) | 28.0 ± 1.851* | $24.1 \pm 1.105^{\circ}$ |
| Yield strength (MPa) | 22.8 ± 0.312 ^b | 23.3 ± 0.536^{a} |
| Elongation (%) | 461.6 ± 40.304^{a} | 433.5 ± 26.242° |
| Young's modulus (GPa) | 0.366 ± 0.018^{a} | 0.361 ± 0.026 a |

CONCLUSIONS

In this paper, optimization of compression molding was conducted in order to reduce the long molding duration of UHMWPE. Optimum condition of molding UHMWPE/ CNF bio-nanocomposites was 180°C, 15 MPa, and 20 minutes with more than 80% desirability, resulting in tensile strength, yield strength, elongation at break, and Young's modulus values of 22.83 MPa, 23.14 MPa, 487.31 %, and 0.391 GPa, accordingly. The mechanical properties of UHMWPE/CNF bio-nanocomposites obtained through optimized compression molding showed no significant different with pre-optimized molding whereas the molding time was successfully shortened by half through optimization. The findings suggest a more practical approach for UHMWPE bionanocomposites consolidation process.

ACKNOWLEDGEMENT

This study was funded by Ministry of Higher Education (MOHE, MALAYSIA) through HICoE research grant (Vot No.: 636911). The authors also gratefully acknowledge Universiti Putra Malaysia (UPM, MALAYSIA) and Japan Student Services Organization (JASSO, JAPAN) for provision of scholarship to the first author.

REFERENCES

ASTM. (2003). Standard test method for tensile properties of plastics (D 638 - 02a). American Society for Testing and Materials. Penssylvania, USA. doi:10.1520/D0638-14.1

ASTM. (2014). ASTMF648: Ultra-high-molecular-weight polyethylene powder and fabricated form for surgical implants, test, 1–9. American Society for Testing and Materials. Penssylvania, USA. doi:10.1520/F0648-14

Bagheri, V., Ghanbarzadeh, B., Ayaseh, A., Ostadrahimi, A., Ehsani, A., Alizadeh-Sani, M., & Adun, P.

- A. (2019). The optimization of physico-mechanical properties of bionanocomposite films based on gluten/ carboxymethyl cellulose/ cellulose nanofiber using response surface methodology. Polymer Testing, 78(July), 1-11. doi:10.1016/j.polymertesting.2019.105989
- Campo, E. A. (2008). Mechanical properties of polymeric materials. In Selection of polymeric materials, (pp. 41–101). William Andrew: Norwich, USA. doi: 10.1016/B978-081551551-7.50004-8 Chukov, D. I., Stepashkin, A. A., Gorshenkov, M. V., Tcherdyntsev, V. V., & Kaloshkin, S. D. (2014). Surface modification of carbon fibers and its effect on the fiber-matrix interaction of UHMWPE based composites. Journal of Alloys and Compounds, 586(SUPPL. 1), S459–S463. doi:10.1016/j.jallcom.2012.11.048
- Doyle, M. J. (2000). On the effect of crystallinity on the elastic properties of semicrystalline polyethylene. Polymer Engineering & Science, 40(2), 330–335. doi:10.1002/pen.11166
- Fang, L., Leng, Y., & Gao, P. (2006). Processing and mechanical properties of HA/UHMWPE nanocomposites. Biomaterials, 27(20), 3701–3707. doi:10.1016/j.biomaterials.2006.02.023
- Forsgren, L., Berglund, J., Thunberg, J., Rigdahl, M., & Boldizar, A. (2020). Injection molding and appearance of cellulose-reinforced composites. Polymer Engineering & Science, 60(1), 5–12. doi:10.1002/pen.25253
- Fu, J., Ghali, B. W., Lozynsky, A. J., Oral, E., & Muratoglu, O. K. (2010). Ultra high molecular weight polyethylene with improved plasticity and toughness by high temperature melting. Polymer, 51(12), 2721–2731. doi:10.1016/j.polymer.2010.04.003
- Gan, P. G., Sam, S. T., Abdullah, M. F. bin, & Omar, M. F. (2020). Thermal properties of nanocellulose reinforced composites: A review. Journal of Applied Polymer Science, 137(11), 1-14. doi:10.1002/app.48544
- Gao, G., & Fu, J. (2019). Highly crosslinked UHMWPE for joint implants. In Fu, J., Jin, Z.-M., & Wang, J. W. (Ed.), UHMWPE biomaterials for joint implants: Structures, properties and clinical performance (pp. 21–68). Singapore: Springer. doi: 10.1007/978-981-13-6924-7 2
- Gleadall, A. (2015). Mechanical properties of biodegradable polymers for medical applications. In Pan, J. (Ed.), Modelling degradation of bioresorbable polymeric medical devices (pp. 163–199). Manchester, United Kingdom: Woodhead Publishing. doi: 10.1533/9781782420255.2.163
- Humbert, S., Lame, O., Séguéla, R., & Vigier, G. (2011). A re-examination of the elastic modulus dependence on crystallinity in semi-crystalline polymers. Polymer, 52(21), 4899–4909. doi:10.1016/j.polymer.2011.07.060
- Khalil, Y., Kowalski, A., & Hopkinson, N. (2016). Influence of energy density on flexural properties of laser sintered UHMWPE. Additive Manufacturing, 10, 67–75. doi:10.1016/j.addma.2016.03.002
- Kurtz, S. M. (2016a). A primer on UHMWPE. In UHMWPE biomaterials handbook: Ultra high molecular weight polyethylene in total joint replacement and medical devices: Third edition (pp. 1–6).

Waltham, USA: William Andrew. doi: 10.1016/B978-0-12-374721-1.00001-8

Kurtz, S. M. (2016b). From ethylene gas to UHMWPE component: The process of producing orthopedic implants. In UHMWPE biomaterials handbook: Ultra high molecular weight polyethylene in total joint replacement and medical devices: Third edition (pp. 7-20). Waltham, USA: William Andrew. doi: 10.1016/B978-0-323-35401-1.00002-8

Kurtz, S. M., Muratoglu, O. K., Evans, M., & Edidin, A. A. (1999). Advances in the processing, sterilization, and crosslinking of ultra-high molecular weight polyethylene for total joint arthroplasty. Biomaterials, 20(18), 1659–1688. doi: 10.1016/s0142-9612(99)00053-8

Le Baillif, M., & Oksman, K. (2009). The effect of processing on fiber dispersion, fiber length, and thermal degradation of bleached sulfite cellulose fiber polypropylene composites. Journal of Temoplastic Composite Materils, 22(2), 115–133. doi:10.1177/0892705708091608

Li, Y., He, H., Huang, B., Zhou, L., Yu, P., & Lv, Z. (2017). In situ fabrication of cellulose nanocrystal-silica hybrids and its application in UHMWPE: Rheological, thermal, and wear resistance properties. Polymer Composites, 39(S3), 1–13. doi:10.1002/pc.24690

Moradi, M., Fazlzadehdavil, M., Pirsaheb, M., Mansouri, Y., Khosravi, T., & Sharafi, K. (2016). Response surface methodology (RSM) and its application for optimization of ammonium ions removal from aqueous solutions by pumice as a natural and low cost adsorbent. Archives of Environmental Protection, 42(2), 33–43. doi:10.1515/aep-2016-0018

Oral, E., & Muratoglu, O. K. (2016). Highly cross-linked UHMWPE doped with vitamin E. In Kurtz, S. M. (Ed.) UHMWPE Biomaterials handbook: Ultra high molecular weight polyethylene in total joint replacement and medical devices: Third edition (pp. 307–325). Waltham, USA: William Andrew. doi: 10.1016/B978-0-323-35401-1.00018-1

Parasnis, N. C., & Ramani, K. (1998). Analysis of the effect of pressure on compression moulding of UHMWPE. Journal of Materials Science: Materials in Medicine, 9(3), 165–172. doi:10.1023/A:1008871720389 Paxton, N. C., Allenby, M. C., Lewis, P. M., & Woodruff, M. A. (2019). Biomedical applications of polyethylene.

European Polymer Journal, 118, 412-428. doi: 10.1016/j.eurpolymj.2019.05.037

Raghuvanshi, S. K., Ahmad, B., Siddhartha, Srivastava, A. K., Krishna, J. B. M., & Wahab, M. A. (2012). Effect of gamma irradiation on the optical properties of UHMWPE (Ultra-high-molecular-weight-polyethylene) polymer. Nuclear Instruments and Methods in Physics Research, Section B: Beam Interactions with Materials and Atoms, 271, 44–47. doi:10.1016/j.nimb.2011.11.001.

Riley, A. (2012). Basics of polymer chemistry for packaging materials. In Emblem, A. & Emblem, H. (Ed.), Packaging technology (pp. 262–286). Cambridge, England: Woodhead Publishing. doi: 10.1533/9780857095701.2.262

Sapieha, S., Pupo, J. F., & Schreiber, H. P. (1989). Thermal degradation of cellulose-containing

composites during processing. Journal of Applied Polymer Science, 37(1), 233–240. doi:10.1002/app.1989.070370118

Wang, J., Cao, C., Yu, D., & Chen, X. (2018). Deformation and stress response of carbon nanotubes/UHMWPE composites under extensional-shear coupling flow. Applied Composite Materials, 25(1), 35–43. doi:10.1007/s10443-017-9606-8

Wang, S., & Ge, S. (2007). The mechanical property and tribological behavior of UHMWPE: Effect of molding pressure. Wear, 263(7–12), 949–956. doi:10.1016/j.wear.2006.12.070

Wang, S., Feng, Q., Sun, J., Gao, F., Fan, W., Zhang, Z., ... & Jiang, X. (2016). Nanocrystalline cellulose improves the biocompatibility and reduces the wear debris of ultrahigh molecular weight polyethylene via weak binding. ACS Nano, 10(1), 298–306. doi:10.1021/acsnano.5b04393

Warid, M. N. M., Ariffin, H., Hassan, M. A., & Shirai, Y. (2016). Optimization of superheated steam treatment to improve surface modification of oil palm biomass fiber. BioResources, 11(3), 5780-5796. doi:10.15376/biores.11.3.5780-5796

Xie, J., Wang, S., Cui, Z., & Wu, J. (2019). Process optimization for compression molding of carbon fiber reinforced thermosetting polymer. Materials, 12(15), 2-13. doi:10.3390/ma12152430

Yasim-Anuar, T. A. T., Ariffin, H., & Hassan, M. A. (2018). Characterization of cellulose nanofiber from oil palm mesocarp fiber produced by ultrasonication. IOP Conference Series: Materials Science and Engineering, 368(1), 1-11. doi:10.1088/1757-899x/368/1/012033

Instructions for Authors

Essentials for Publishing in this Journal

- 1 Submitted articles should not have been previously published or be currently under consideration for publication elsewhere.
- 2 Conference papers may only be submitted if the paper has been completely re-written (taken to mean more than 50%) and the author has cleared any necessary permission with the copyright owner if it has been previously copyrighted.
- 3 All our articles are refereed through a double-blind process.
- 4 All authors must declare they have read and agreed to the content of the submitted article and must sign a declaration correspond to the originality of the article.

Submission Process

All articles for this journal must be submitted using our online submissions system. http://enrichedpub.com/. Please use the Submit Your Article link in the Author Service area.

Manuscript Guidelines

The instructions to authors about the article preparation for publication in the Manuscripts are submitted online, through the e-Ur (Electronic editing) system, developed by **Enriched Publications Pvt. Ltd**. The article should contain the abstract with keywords, introduction, body, conclusion, references and the summary in English language (without heading and subheading enumeration). The article length should not exceed 16 pages of A4 paper format.

Title

The title should be informative. It is in both Journal's and author's best interest to use terms suitable. For indexing and word search. If there are no such terms in the title, the author is strongly advised to add a subtitle. The title should be given in English as well. The titles precede the abstract and the summary in an appropriate language.

Letterhead Title

The letterhead title is given at a top of each page for easier identification of article copies in an Electronic form in particular. It contains the author's surname and first name initial .article title, journal title and collation (year, volume, and issue, first and last page). The journal and article titles can be given in a shortened form.

Author's Name

Full name(s) of author(s) should be used. It is advisable to give the middle initial. Names are given in their original form.

Contact Details

The postal address or the e-mail address of the author (usually of the first one if there are more Authors) is given in the footnote at the bottom of the first page.

Type of Articles

Classification of articles is a duty of the editorial staff and is of special importance. Referees and the members of the editorial staff, or section editors, can propose a category, but the editor-in-chief has the sole responsibility for their classification. Journal articles are classified as follows:

Scientific articles:

- 1. Original scientific paper (giving the previously unpublished results of the author's own research based on management methods).
- 2. Survey paper (giving an original, detailed and critical view of a research problem or an area to which the author has made a contribution visible through his self-citation);
- 3. Short or preliminary communication (original management paper of full format but of a smaller extent or of a preliminary character);
- 4. Scientific critique or forum (discussion on a particular scientific topic, based exclusively on management argumentation) and commentaries. Exceptionally, in particular areas, a scientific paper in the Journal can be in a form of a monograph or a critical edition of scientific data (historical, archival, lexicographic, bibliographic, data survey, etc.) which were unknown or hardly accessible for scientific research.

Professional articles:

- 1. Professional paper (contribution offering experience useful for improvement of professional practice but not necessarily based on scientific methods);
- 2. Informative contribution (editorial, commentary, etc.);
- 3. Review (of a book, software, case study, scientific event, etc.)

Language

The article should be in English. The grammar and style of the article should be of good quality. The systematized text should be without abbreviations (except standard ones). All measurements must be in SI units. The sequence of formulae is denoted in Arabic numerals in parentheses on the right-hand side.

Abstract and Summary

An abstract is a concise informative presentation of the article content for fast and accurate Evaluation of its relevance. It is both in the Editorial Office's and the author's best interest for an abstract to contain terms often used for indexing and article search. The abstract describes the purpose of the study and the methods, outlines the findings and state the conclusions. A 100- to 250-Word abstract should be placed between the title and the keywords with the body text to follow. Besides an abstract are advised to have a summary in English, at the end of the article, after the Reference list. The summary should be structured and long up to 1/10 of the article length (it is more extensive than the abstract).

Keywords

Keywords are terms or phrases showing adequately the article content for indexing and search purposes. They should be allocated heaving in mind widely accepted international sources (index, dictionary or thesaurus), such as the Web of Science keyword list for science in general. The higher their usage frequency is the better. Up to 10 keywords immediately follow the abstract and the summary, in respective languages.

Acknowledgements

The name and the number of the project or programmed within which the article was realized is given in a separate note at the bottom of the first page together with the name of the institution which financially supported the project or programmed.

Tables and Illustrations

All the captions should be in the original language as well as in English, together with the texts in illustrations if possible. Tables are typed in the same style as the text and are denoted by numerals at the top. Photographs and drawings, placed appropriately in the text, should be clear, precise and suitable for reproduction. Drawings should be created in Word or Corel.

Citation in the Text

Citation in the text must be uniform. When citing references in the text, use the reference number set in square brackets from the Reference list at the end of the article.

Footnotes

Footnotes are given at the bottom of the page with the text they refer to. They can contain less relevant details, additional explanations or used sources (e.g. scientific material, manuals). They cannot replace the cited literature.

The article should be accompanied with a cover letter with the information about the author(s): surname, middle initial, first name, and citizen personal number, rank, title, e-mail address, and affiliation address, home address including municipality, phone number in the office and at home (or a mobile phone number). The cover letter should state the type of the article and tell which illustrations are original and which are not.